DNA repair in kidney development and Wilms tumor

Leah Hammond

Department of Human Genetics, Faculty of Medicine

McGill University, Montreal, Quebec, Canada

August, 2018

A thesis submitted to McGill University in partial fulfillment of the requirements of the degree of Master of Science

ABSTRACT

DNA repair is of particular importance in the rapidly-dividing progenitor cells of developing organs. Unrepaired damage in these cells may disrupt embryonic development and be propagated throughout an entire cell lineage of the adult organ. We hypothesize that specific DNA repair programs are activated during embryogenesis to protect the genome in this critical phase and that, in the developing kidney, a panel of DNA repair genes are activated to accompany the burst of cell division during nephrogenesis. Furthermore, we hypothesize that activation of a subset of the DNA repair genes in nephron progenitor cells (NPCs) is elicited by Wilms Tumor 1 (WT1) and therefore loss of WT1 might compromise DNA repair in the developing kidney. Loss of WT1 from NPCs is known to cause clones of developmentally-arrested cells that carry a high risk of acquiring activating mutations of the *CTNNB1* gene. Constitutive *CTNNB1* activation is associated with malignant transformation into a Wilms tumor. However, the mechanism underlying this apparent genomic instability of NPCs, following loss of WT1, is unknown.

In this project, we quantified the expression of 84 DNA repair genes in embryonic versus adult mouse kidney. We identified 7 genes with a 20-fold or greater upregulation in the embryo compared to the adult. To isolate NPCs from the embryonic mouse kidney, we used a transgenic mouse model consisting of *Cited1*-driven Cre recombinase crossed with a tdTomato reporter strain. Using Reverse Transcription quantitative Polymerase Chain Reaction (RT-qPCR), we showed that expression of the DNA repair gene *Neil3* was 15-fold higher in NPCs compared to total kidney. When we examined *Neil3* expression in another rapidly-dividing embryonic kidney lineage, the *Hoxb7*/GFP-tagged ureteric bud lineage, we saw no enrichment relative to total kidney.

We adapted our *Cited1*-driven Cre recombinase system to allow isolation of NPCs carrying an inducible *Wt1* knockout mutation. Using RT-qPCR, we confirmed that enrichment of *Neil3* in NPCs with conditional ablation of *Wt1* was reduced by 60% compared to NPCs with wildtype *Wt1*. We propose that WT1-mediated activation of a DNA repair program that may include *Neil3* is critical for maintaining genomic stability

in rapidly-proliferating NPCs. Loss of this DNA repair activity could contribute to development of the activating mutations driving Wilms tumor.

RÉSUMÉ

La réparation de l'ADN est particulièrement importante pour les cellules progénitrices qui se divisent rapidement pour former les organes. Les dommages qui n'ont pas été réparées dans ces cellules peuvent perturber le développement embryonnaire et être propagées à travers tout l'organe. Notre hypothèse est que des programmes de réparation d'ADN sont activés durant l'embryogénèse afin de protéger le génome durant cette phase cruciale. Lors du développement rénal, une panoplie de gènes de réparation de l'ADN est activée pendant la période de division rapide de la néphrogénèse. De plus, nous proposons qu'il y a un sous-ensemble des gènes responsables de la réparation de l'ADN qui est activé dans les cellules rénales progénitrices (NPCs) et que celui-ci dépend du gène suppresseur de tumeur de Wilms*, WT1*. Nous formulons l'hypothèse que la perte de WT1 compromet l'activation du système de réparation de l'ADN qui protège normalement les NPCs. La perte de WT1 dans les NPCs génère des clones de cellules dont le développement a été interrompu. Ces clones ont un risque élevé d'incorporation des mutations activantes du gène *CTNNB1*. L'activation constante de ce dernier est associée à la transformation maligne en tumeur de Wilms. Le mécanisme qui sous-tend cette apparente instabilité génomique des NPCs, suivant la perte de WT1, est inconnu.

Dans cette étude, nous quantifions l'expression de 84 gènes de réparation de l'ADN dans les reins embryonnaires et adultes, chez la souris. Nous avons identifié 7 gènes dont l'expression était au moins 20 fois plus élevée dans embryon que dans adulte. Pour isoler les NPCs, nous avons utilisé un modèle de souris transgénique dont la Cre recombinase est contrôlée par le promoteur de *Cited1* croisé avec une lignée de souris qui possèdent le gène rapporteur *tdTomato*. En utilisant la réaction en chaîne de la polymérase de transcription inverse quantitative (RT-qPCR), nous avons observé que l'expression du gêne de réparation *Neil3* était 15 fois plus élevé dans les NPCs par rapport au rein dans son ensemble. Lorsque nous avons examiné l'expression de *Neil3* dans une autre lignée cellulaire de reins embryonnaires dérivée du bourgeon urétéral marquée par *Hoxb7*/GFP, nous n'avons pas observé une telle augmentation.

Nous avons adapté notre système *Cited-1*/Cre recombinase afin de permettre l'isolation de NPCs qui possèdent une mutation knock-out inductible de *Wt1*. En utilisant la RT-qPCR, nous avons confirmé que l'enrichissement de *Neil3* dans NPCs avec l'ablation conditionnelle de *Wt1* est réduit de 60% par rapport aux NPCs sans l'ablation. Nous proposons que l'activation du programme de réparation de l'ADN dépendant de WT1, qui peut inclure *Neil3*, est critique pour maintenir une stabilité génomique dans les NPCs en prolifération rapide. La perte de cette activité de réparation de l'ADN peut contribuer au développement des mutations activantes qui causent les tumeurs de Wilms.

TABLE OF CONTENTS

ABBREVIATIONS

4OHT	4-Hydroxytamoxifen
8-oxoG	8-Oxoguanine
AP Site	apurinic/apyrimidic site
B2M	beta-2 microglobulin
BAC	bacterial artificial chromosome
BER	base excision repair
BMP7	bone morphogenetic protein 7
BRCA1	breast cancer gene 1
BRCA2	breast cancer gene 2
C->T	cytosine to thymine
cDNA	complementary DNA
ChIP/ChIP-SEQ	chromatin immunoprecipitation/chromatin immunoprecipitation-sequencing
CITED1	Cbp/p300 interacting transactivator with Glu/Asp rich carboxy-terminal domain 1
CM	cap mesenchyme
CO_2	carbon dioxide
C_T	cycle threshold
CTNNB1	beta-catenin gene 1
DMEM	Dulbecco's Modified Eagle Medium
DNA	deoxyribonucleic acid
DNase 1	deoxyribonuclease 1
DSB	double-stranded break
E(as in E17.5)	embryonic day
EDTA	ethylenediaminetetraacetic acid
EXO1	exonuclease 1
FACS	fluorescence-activated cell sorting
FBS	fetal bovine serum
GFP	green fluorescent protein
GUDMAP	GenitoUrinary Development Molecular Anatomy Project
HOXB7	homeobox B7
HR	homologous recombination
ITS	insulin-transferrin-selenium
KTS	Lysine-Threonine-Serine
LIG1	DNA ligase I
mRNA	messenger RNA
MET	mesenchymal-to-epithelial transition
MMR	mismatch repair
MSI	microsatellite instabilty
NEIL3	nei like DNA glycosylase 3
NER	nucleotide excision repair

NHEJ	non-homologous end joining
NPC	nephron progenitor cell
OSR1	odd-skipped related transciption factor 1
PARP3	poly (ADP-ribose) polymerase family, member 3
PAX2	paired box 2
PBS	phosphate-buffered saline
PFA	paraformaldehyde
qPCR	quantitative polmerase chain reaction
R26	Gt(ROSA)26Sor locus
RAD18	RAD18 E3 ubiquitin protein ligase
RAD51B	RAD51 paralog B
RAD54B	RAD54 homolog B
RNA	ribonucleic acid
RNase	ribonuclease
RPM	revolutions per minute
RT-qPCR	reverse transcription quantitative polymerase chain reaction
SALL1	spalt like transcription factor 1
SALL2	spalt like transcription factor 2
SIX1	sine oculis homeobox homolog 1
SIX2	sine oculis-related homeobox 2
TCF/LEF	T-cell factor/lymphoid enhancer factor
TP53	tumor protein p53
UB	ureteric bud
UNG	uracil DNA glycosylase
UV	ultraviolet
WAGR	Wilms tumor, Aniridia, Genitourinary malformation and mental Retardation
WNT	Homolog of the Drosophila wingless-type gene
WT1	Wilms tumor 1

LIST OF FIGURES

LIST OF TABLES

ACKNOWLEDGEMENTS

Please bear with me while I thank the many people who have aided and encouraged me through all the blood (mostly mouse), sweat (mostly mine), and tears (definitely all mine) that this project entailed.

Thank you to members of my supervisory committee, Dr. Yamanaka and Dr. Rak, for devoting time to thoroughly contemplate my project and its direction. Thank you to my supervisor, Paul Goodyer, for your immense warmth, your open-mindedness and your passion for telling a story well. Thanks for always celebrating small successes and remaining calm in the face of setbacks.

PG lab members, I owe each of you a tremendous, emphatic, lab-shaking thank you. Kyle, I had so much fun helping out as your summer student all those years ago that I just had to come back for more! Thank you especially for your patience in teaching me how to dissect out embryonic kidneys and make cryosections. Murielle, it is true that your music made us the peppiest lab around, but you also provided invaluable scientific assistance during this project. Thanks for your help editing several sections of this thesis, and for your expert guidance in the translation of my abstract into French. Thanks for taking me under your wing, showing me the ropes, and demonstrating how to design a truly beautiful qPCR plate. Thanks to both Murielle and Lee Lee for helping me troubleshoot and analyze data. Additionally, thanks to Lee Lee for making sure I always had what I needed (despite endless credit card hassles), and for spending so much time helping me fiddle with the fluorescent microscope settings. Thanks to Emma for asking thoughtful questions about experimental design and guiding me on all McGill Human Genetics Department matters (along with Ross MacKay, of course). Thanks to Sarah for your camaraderie and company in the mouse room. Thanks to Fatima, for your guidance in how to use the slightly-more-cooperative fluorescent microscopes, for your help with Microsoft Word formatting nightmares, and for being a cheerleader to so many fellow graduate students. Thanks to Jung Hwa, for your generous help with immunofluorescence microscopy (not included in this thesis), and for your encouragement. Thanks to Rachel, for helping design the mouse

breeding schemes and for supervising some of the early crossings. Thanks to the summer students, Caleb and Alexandre, for being so eager to contribute. Thanks to Mel and Thomas for fascinating, entertaining, and always scientific discussions.

A large part of this project depended on FACS isolation of specific embryonic kidney cells. This could not have been done without many hours of work from the staff at the MUHC Research Institute Immunophenotyping Platform, Ekaterina Iourtchenko and Marie-Hélène Lacombe.

The staff of the Glen Research Institute Animal Resource Division was also invaluable during preparation of this thesis. The vets and technicians devote such energy and dedication to caring for the many animals in the facility, animals without which we would have no projects. In a similar vein, thank you to my mice, who made the ultimate sacrifice for this study.

To my friends (including some new friends within the Human Genetics department), you are helpful in all aspects of life, not just genetics. Finally, thanks to my family for promising to love me even if I failed to single-handedly cure kidney cancer. I still love you too.

PREFACE AND CONTRIBUTIONS OF AUTHORS

This thesis was prepared in adherence to the traditional thesis format outlined by McGill University's Faculty of Graduate and Postdoctoral Studies. The candidate carried out all the experiments described here. Data analysis for the RT-qPCR experiments was performed by the candidate, with assistance from Lee Lee Chu, Dr. Murielle Akpa and Dr. Paul Goodyer. Dr. Murielle Akpa also helped edit several chapters of this thesis. Collection of fluorescent cells by FACS was performed by Ekaterina Iourtchenko and Marie-Hélène Lacombe staff at the MUHC Research Institute Immunophenotyping Platform. Confocal images were taken with assistance from Shi-Bo Feng at the MUHC Research Institute Molecular Imaging Platform. Caleb Tse Lalonde and Alexandre Goumba assisted with some of the early mouse dissections, RNA extractions and PCR genotyping.

CHAPTER 1: INTRODUCTION

In the developing kidney, loss of the transcription factor Wilms Tumor 1 (WT1) from nephron progenitor cells (NPCs) blocks the mesenchymal-epithelial transition (MET) and predisposes these developmentally-arrested cells to oncogenic mutations, such as constitutive-activation of the beta-catenin protein [1-3]. The mechanism linking WT1-loss and cancer predisposition has eluded researchers for many years. It has been well-established in literature that deficient DNA repair can result in genome instability and cancer [4]. In other cancers, DNA repair deficiency has even been linked to the specific constitutively-activating mutations observed in Wilms tumors [5, 6]. The challenge for this project was to determine whether deficient DNA repair might be implicated in the relationship between loss of WT1 from NPCs and the development of oncogenic mutations that frequently follows. Before embarking on the full account of this research, it is necessary to frame our hypothesis by beginning with a brief overview of how kidneys develop in mammals.

1.1 Overview of Mammalian Kidney Development

The mammalian kidney develops from a pool of intermediate mesodermal cells expressing the gene *OSR1* [7]. At embryonic day 10.5 (E10.5) in mice, an outgrowth from the Wolffian Duct, called the ureteric bud (UB), induces mesenchymal cells around its tip to condense and form a cap expressing the genes *Six2* and *Cited1* [8, 9]. The UB continues to outgrow and branch throughout kidney development and expresses the marker gene *Hoxb7* [10]. The UB eventually gives rise to the renal collecting duct system, responsible for collecting the urine formed in the kidney prior to its transport to the bladder [10-12].

In response to a WNT differentiation signal secreted from the UB, NPCs within the Cap Mesenchyme (CM) undergo a MET and form pre-tubular aggregates. Each pre-tubular aggregate forms a renal vesicle, which progresses through a comma-shaped body and S-shaped body stage before eventually giving rise to a mature nephron [13]. Figure 1, taken from [14] illustrates these stages of kidney development. Nephrons represent the filtering

unit of the kidney; humans must produce up to 1 million nephrons over the course of kidney development [15]. Nephrons are complex structures, consisting of several integral components. The important and distinct functions of these components collectively ensures that the correct pH, salt and water levels are maintained in the blood, and that only waste products, and not blood cells or important proteins, are excreted into the urine [15, 16]. Many different specialized epithelial cells are required to form each of these nephron components. The nephron progenitors within the CM are the multipotent cells taxed with generating all the epithelial cells necessary to make up the many hundreds of thousands of nephrons in the adult kidney.

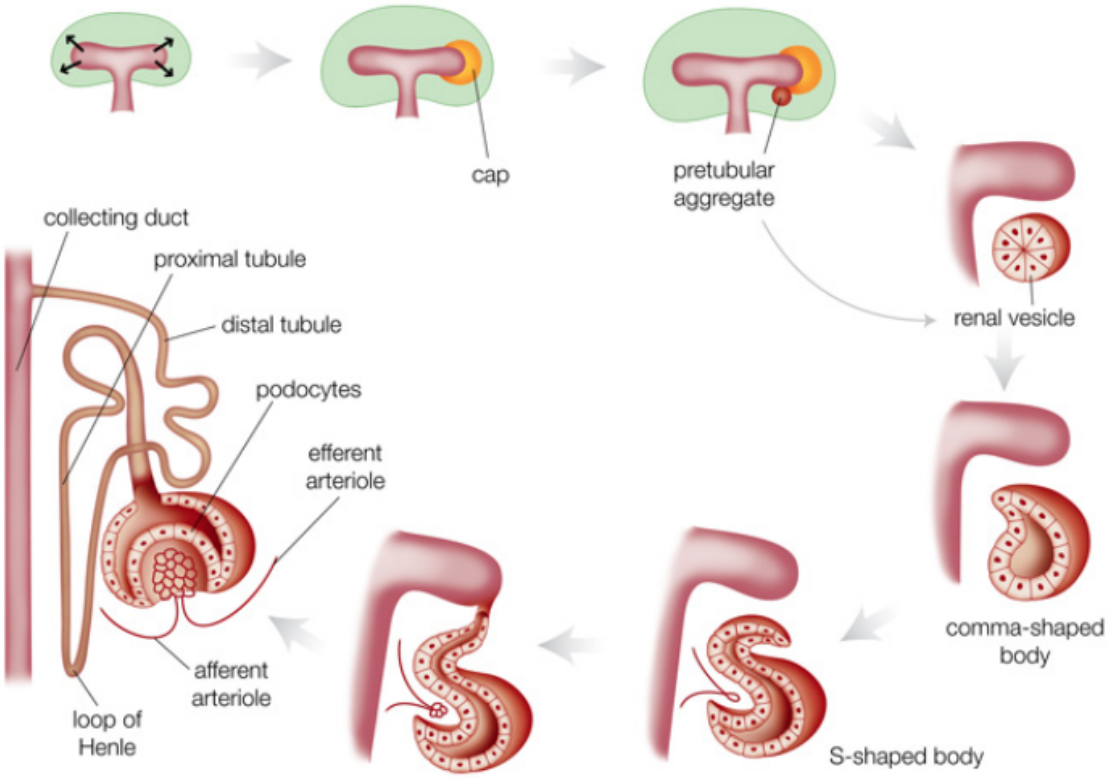

Figure 1. Schematic representation of mammalian kidney development.

WNT9B secreted from the ureteric bud (pink), induces cells in the surrounding mesenchyme (green) to condense and form a clustered cap (orange) around the bud tip. A subset of cells within the cap mesenchyme epithelialize to form a pretubular aggregate and renal vesicle (red). Cells in the renal vesicle undergo rapid proliferation and differentiation, and the vesicle elongates, passing through comma-shaped body and S-shaped body stages before attaching to the ureteric bud at distal end and, ultimately, forming a functional nephron (as depicted in the leftmost bottom corner of the image). Reprinted with permission from [14].

1.2 Defining the Cap Mesenchyme and the Nephron Progenitor Pool

It was shown by Kobayashi et al. in 2008 that expression of *Six2* within the mouse CM is required to prevent premature onset of differentiation and formation of ectopic renal vesicles [17]. Kobayashi et al. argued that *Six2* helps to maintain a pool of undifferentiated nephron progenitors within the CM by blocking the WNT9B signal secreted from the ureteric bud. WNT9B would otherwise direct the NPCs to differentiate and epithelialize.

Cited1 expression overlaps with that of *Six2* in the developing mouse kidney, however it is only expressed in the most lateral portion of the CM, while *Six2* is expressed broadly throughout the CM, including in the clefts of the UB branch points [18]. Additionally, it was shown by Brown et al. in 2013 that loss of *Cited1* expression from a subset of *Cited1*+/*Six2*+ CM cells is necessary for nephron progenitors to become competent to respond to the WNT9B signal [19]. It is therefore the simultaneous expression of both *Cited1*+ and *Six2*+ that defines the self-renewing nephron progenitor pool of the CM; the cells that lose *Cited1* expression subsequently define the NPC subset that can be induced to epithelialize.

1.3 Canonical WNT Signaling

1.3.1 Canonical WNT Signaling During Kidney Development

The family of secreted glycoproteins known as WNTs can bind to cell surface receptors and activate several potential pathways within the cell. Canonical WNT signaling is mediated by stabilization of the beta-catenin protein, which then accumulates in the cytoplasm, enters the nucleus and, together with TCF/Lef proteins, activates transcription of numerous downstream targets [20]. In the absence of a WNT ligand binding to a receptor at the cell surface, the cell normally turns over cytoplasmic beta-catenin quite rapidly. This rapid turnover is accomplished by a degradation complex that phosphorylates beta-catenin at critical residues, thereby tagging the protein for ubiquitination and degradation.

Canonical WNT signaling has been implicated in such diverse cellular processes as survival, motility, proliferation, and differentiation [20], and previous studies have demonstrated a clear role for beta-catenin-mediated WNT signaling specifically during nephrogenesis [21, 22]. In a comprehensive review of WNT signaling during kidney development, Holt and Vainio argue that WNT9B and WNT4 are the two most important WNTs involved in kidney organogenesis [21]. WNT9B was identified by Carroll et al. as the primary inductive signal required to initiate the formation of pre-tubular aggregates [23]. WNT4 is a marker of the pre-tubular aggregates induced by WNT9B and is necessary and sufficient for induction of renal vesicle formation, even in the absence of WNT9B [23]. Transgenic expression of *Wnt1* in the UB of *Wnt9b-/-* mice is sufficient to rescue the *Wnt9b-/-* phenotype. As WNT1 is believed to only participate in canonical WNT signaling, this suggests that the ability of WNT9B and WNT4 to drive tubulogenesis in the kidney is mediated specifically through canonical WNT signaling pathways. Subsequent studies by our lab have since confirmed this concept [22].

1.3.2 Canonical WNT Signaling in Cancer

Constitutive activation of canonical WNT signaling has been described in several cancers, including hepatocellular carcinoma [24, 25], colorectal cancer [26] and, as will be a principle point of discussion in this thesis, Wilms tumor [1-3]. A review of WNT signaling in disease by Moon et al. [27] discusses how the concentration of numerous repressor proteins on the beta-catenin-dependant WNT signaling pathway demonstrates the importance of this pathway's regulation. Indeed, because downstream targets of this pathway control cell proliferation, it is evident that dysregulation of this pathway has oncogenic potential.

Constitutive activation of the canonical signaling pathway can be achieved via several mechanisms: as is seen in many colorectal cancers, a component of the beta-catenin degradation complex can be defective [28]; alternatively, as is seen in hepatocellular carcinomas, some colorectal cancers and many Wilms tumors, mutations at critical phosphorylation sites of beta-catenin can prevent the protein from being phosphorylated

and subsequently degraded [1-3, 24, 26]. The occurrence of beta-catenin-stabilizing mutations in Wilms tumors is discussed in greater detail in section **1.5** of this thesis.

1.4 Wilms Tumor 1

1.4.1 Wilms Tumor 1 in Kidney Development

WT1 encodes a zinc-finger transcription factor that is required for normal mammalian kidney development [29]. In the earliest studies of this gene, *Wt1* null mice died during embryogenesis and failed to form kidneys. While it is the kidney phenotype that is of interest in this project, expression of *Wt1* in the gonads, spleen, epicardium and mesothelial lining of the abdominal cavity is important for directing development within these structures/tissues of vertebrate embryos [30]. In the *Wt1-/-* mouse embryos, the UB did not invade the metanephric mesenchyme, and the mesenchyme underwent apoptosis [29]. It was shown through co-culture experiments that apoptosis of the metanephric mesenchyme in *Wt1-/-* embryos was due to lack of *Wt1* and was not a downstream effect of failed UB invasion. Wildtype UB was unable to induce *Wt1-/-* metanephric mesenchymal rudiments to differentiate and form tubules [31], yet wildtype mesenchymal rudiments were inducible by spinal cord and underwent tubule differentiation [29].

The early embryonic lethality of constitutive *Wt1* knockout was an obstacle to researchers hoping to study the function of *Wt1* beyond the earliest stages of embryogenesis. This obstacle has since been overcome with the advent of two techniques: (i) the use of small interfering RNAs that knockdown *Wt1* expression and can be administered at specific developmental timepoints; (ii) the creation of transgenic mice using the Cre/lox recombination system to induce *Wt1* mutations only at specific developmental stages and within certain cell types of the embryonic mouse kidney [32, 33]. Studies using these techniques have shown that *Wt1* serves several distinct and crucial roles during kidney development and in the mature kidney.

At the onset of kidney formation, *Wt1* is expressed weakly throughout the metanephric mesenchyme. Knockout of *Wt1* expression from this early stage of organogenesis

mimics the phenotype of *Wt1-/-* mice and demonstrates a role for *Wt1* in survival of the metanephric mesenchyme and induction of branching and outgrowth in the adjacent UB [32]. The expression of *Wt1* increases specifically in the NPCs contained within the CM as development proceeds. *Wt1* is required for directing the mesenchymal-epithelial transition (MET) of NPCs in the CM, and subsequently, *Wt1* is necessary for tubule formation by these cells. Consistent with a role for *Wt1* during differentiation of NPCs, it has been shown that several genes implicated in nephrogenesis, including *Bmp7, Pax2*, and *Sall1,* are transcriptional targets of WT1 [34]. Previous studies from our lab have shown that expression of *Wt1* in CM cells allows these cells to respond to the WNT9B differentiation signal secreted from the ureteric bud [35]. In the mature nephron, *Wt1* is expressed only in the podocyte cells of the glomerulus, where it is required for normal podocyte function [30, 36].

1.4.2 WT1 as a Master Regulator

Alternative splicing of the *WT1* gene and the use of alternative start codons during translation result in approximately 36 distinct WT1 isoforms [37]. Of these, there are two classes of isoforms discussed most often in literature, resulting from the inclusion/exclusion of Lysine-Threonine-Serine (KTS) between the third and fourth zinc finger. The inclusion of KTS has been shown to change the localization and efficiency of DNA binding and also confer RNA binding ability [38-40]. In addition to binding RNA and DNA, it has also been shown that WT1 participates in a unique chromatin flip-flop mechanism [41], and plays a role in both post-transcriptional [42] and epigenetic regulation [43]. Furthermore, WT1 interacts with many known DNA-binding proteins, which may further designate the activity of WT1 at a specific genomic locus and within a given cellular context [44-47]. The diverse array of mechanisms by which WT1 can regulate expression of targets led Toska and Roberts to label WT1 as a master regulator of organ development [48].

1.4.2.1 WT1 as a DNA-Binding Transcription Factor

Early studies of WT1 as a DNA-binding transcription factor identified a 10 bp motif to which WT1 binds with high affinity *in vitro*. Putative targets of WT1 were identified by

searching for WT1 consensus motifs in the known promoters of genes implicated in cell growth or differentiation processes[49]. Transient reporter transfection assays demonstrated the ability of WT1 to either activate or repress transcription of putative targets *in vitro* [50]. Several of these putative WT1 targets were later validated as true biological targets *in vivo* by experiments that used chromatin immunoprecipitation (ChIP) followed by mouse promoter microarray analysis to identify WT1-bound promoters within embryonic mouse kidney DNA [34]. Subsequently, studies using ChIP followed by sequencing (ChIP-Seq) of WT1-bound fragments identified more WT1 targets and provided further validation of previously-identified target genes [51-53]. Notably, one ChIP-Seq study by Motamedi et al. observed that over 50% of WT1-binding sites were positioned 50-500 kilobases away from the closest transcription start site, implying that the majority of WT1-mediated transcriptional regulation occurs through WT1 binding to distal regulatory elements [53].

1.4.2.2 WT1 as a Post-Transcriptional Regulator

It was shown over 20 years ago that WT1 can bind both DNA and RNA [54]. WT1, particularly the (+KTS) isoform, has also been shown to interact with polysomes, upon which multiple ribosomes converge to translate mRNA [40]. Additionally, WT1 has been implicated in mediating the splicing of transcripts, as the WT1 (+KTS) isoform was shown to interact with key splicing factors and be incorporated into spliceosomes [55, 56]. Recently, WT1 has been shown to regulate a subset of microRNAs, several of which repress translation of proteins involved in control of the NPC differentiation cascade [57]. It is plausible that the regulation of microRNAs represents yet another method of WT1-mediated post-transcriptional regulation.

1.4.2.3 WT1 Influences Epigenetic Regulation

One of the most remarkable characteristics of WT1 is its ability to activate transcription of a given target in one cellular context, and repress transcription of the same target in a different context. The best-described example of this phenomenon is activation of the gene *Wnt4* by WT1 during mesenchymal-to-epithelial of the NPCs during kidney development and repression of *Wnt4* by WT1 during the epithelial-to-mesenchymal

transition of the developing epicardium [41]. ChIP experiments by Essafi et al. showed that WT1 binds to the *Wnt4* promoter in both the developing kidney and epicardium and recruits either a transcriptional coactivator or repressor, in the kidney and heart respectively. Recruitment of transcriptional coactivators or repressors to the *Wnt4* promoter result in activating or repressing histone modifications which designate the transcriptional state of *Wnt4*. Interestingly, the chromatin marks and transcriptional status are reversed (flip-flopped), following loss of WT1 from epicardial cells or cells in the developing kidney [41]. These findings suggest that regulation by WT1 is extremely dependent on cellular context.

Several WT1 transcriptional targets also encode proteins involved in epigenetic regulation of the genome. These targets include DNA methyltransferases [43], histone acetyltransferases [58], and lysine-specific demethylases [58]. By influencing the genome-wide distribution of epigenetic marks, WT1 conceivably has a much farther-reaching affect on transcription than may have once been suggested from analysis of WT1 direct transcriptional targets alone.

1.4.3 *WT1* in Wilms Tumor

WT1 was named for its association with the disease Wilms tumor, which is the most common childhood kidney cancer [59, 60]. Mutations in *WT1* account for up to 20% of Wilms tumor cases [61]. The *WT1* locus was identified through the segregation of deletions at 11p13 with Wilms tumor, aniridia, genitourinary malformation and mental retardation (WAGR) syndrome in children [29]. Subsequently, it was discovered that 90% of patients with Denys-Drash syndrome, characterized by pseudohermaphroditism, nephropathy and Wilms tumor, harbor constitutional *WT1* mutations [62].

Germline mutations in *WT1* are responsible for Wilms' tumor predisposition, however somatic loss of the second *WT1* allele must occur before tumors form; this was first proposed by Knudson in his two-hit model of genetic predisposition to cancer [63]. Indeed, inherited predisposition to Wilms tumor was one of the first cancers studied by Knudson in development of his two-hit model [64]. Somatic loss of the second *WT1*

allele from kidney precursor cells is necessary but insufficient for tumorigenesis; a further activating mutation must occur before Wilms tumors develop. Loss of WT1 from CM cells blocks the MET of NPCs and results in clones of *WT1-/-* undifferentiated cells, referred to as 'nephrogenic rests' [1, 3]. Nephrogenic rests represent cellular pockets of stalled embryonic development in the mature kidney [3]. Nephrogenic rests are considered precursor lesions to Wilms tumors, and are especially prone to developing subsequent oncogenic mutations [1, 3].

1.5 Beta-catenin Mutations in Wilms tumor

Constitutively-activating mutations in the *CTNNB1* gene, encoding beta-catenin, have been described in 15% of Wilms tumor cases. In 2000, a pivotal study by Maiti et al. found a highly significant association between activating mutations in exon 3 of *CTNNB1* and mutations of the *WT1* gene in Wilms tumors [2]. In that study, 95% of tumor samples with somatic *CTNNB1* mutations also had *WT1* inactivating mutations. All of the *CTNNB1* mutations described resulted in loss of key phosphorylation sites from the encoded protein, thereby interfering with the normal degradation of beta-catenin. It was shown that loss of *WT1* precedes mutation of *CTNNB1*, as the tumors' genomes contain the *CTNNB1* mutations, while these mutations are absent from the nephrogenic rests (precursor lesions) [1].

A more recent study sequenced the complete *CTNNB1* coding region in Wilms tumors with *WT1* mutations and described several novel *CTNNB1* mutations outside of the exon 3 'hotspot' region, which resulted in constitutive WNT/beta-catenin pathway activation [65]. Notably, all Wilms tumors with *WT1* mutations that were analyzed in this study showed overexpression of beta-catenin target genes when compared to tumors lacking *WT1* mutations; this included tumors in which no *CTNNB1* mutation could be identified. Based on these findings, the authors concluded that there is a strong selection for activating mutations in the WNT canonical signaling pathway in *WT1-/-* Wilms tumors. Currently, the mechanism is not known by which WT1 loss predisposes cells in the developing kidney to such activating mutations. Intriguingly, this relationship between loss of WT1 and subsequent tumorigenesis seems to be quite specific to a particular cell

type (nephron progenitors) and a narrow window of time during embryonic kidney development. Otherwise, patients with constitutional mutations in *WT1* might be expected to develop Wilms tumors at any point throughout their lifetime, as opposed to presenting with tumors almost exclusively in early childhood, as is clinically observed. Additionally, tumors might be expected to develop in other WT1-expressing tissues (such as the epicardium), following somatic loss of the second *WT1* allele from a cell outside of the developing kidney (this is not observed).

To explore this relationship in mice, Huff and coworkers used Cre recombinase expressed specifically in the NPCs of the embryonic mouse kidney to generate inducible mutations in *Wt1* and *Ctnnb1*. These Cre-mediated mutations occurred only when the embryos were treated *in vivo* with Tamoxifen. The mutations resulted in inactivation of *Wt1* and stabilization of the beta-catenin protein, encoded by *Ctnnb1* [66]. Interestingly, Huff et al. found that stabilization of beta-catenin was sufficient to drive tumor formation, regardless of *Wt1* ablation. Mice with NPC-targeted *Wt1* ablation and beta-catenin stabilization developed tumors at the same age and same rate as mice with only beta-catenin stabilization and functional *Wt1*. This study provided evidence that stabilization of beta-catenin and resulting activation of the WNT/beta-catenin pathway is responsible for driving tumor formation in a subset of Wilms tumors, however it did not address the intermediate steps between loss of *Wt1* from nephron progenitors and development of beta-catenin stabilizing mutations.

1.6 DNA Repair

One plausible explanation for the relationship between WT1 loss from nephron progenitors and WNT/beta-catenin-driven tumorigenesis is that WT1 is important in activating or maintaining DNA repair in the developing kidney, during which time cells are undergoing rapid proliferation. Under this model, loss of WT1 from NPCs would result in dysregulation of DNA repair, and mutations would be expected to arise at an increased frequency. It is possible that mutations promoting cell survival and proliferation (most notably, stabilizing beta-catenin mutations), would be selected for over any silent or deleterious variants [65].

It is known from prior studies that organ development in embryos involves rapid cell proliferation, extensive gene transcription, and a switch from anaerobic to oxidative metabolism, which may result in increased oxidative damage to DNA [67]. It follows that DNA repair is of the utmost importance in cells involved in the organogenesis process. Any unrepaired damage in these cells may be widely propagated throughout the mature organ and may disrupt embryonic development [67-69]. Inactivating mutations in DNA repair genes are often lethal to mice during embryogenesis, underlining the importance of DNA repair during development [70-74].

Expression of certain DNA repair genes has been shown to be specific to both the tissue and developmental stage, perhaps explaining how compromise of particular DNA repair enzymes in a given cellular context can lead to such specific tumor disposition phenotypes (as opposed to a broader genomic instability effect) [75].

Due to the complex consequences of deficient DNA repair and the lesions that accumulate as a result, we did not feel comfortable with *a priori* selection of which repair pathways might be important in Wilms tumor and nephrogenesis. We therefore took a less-biased approach and began by examining expression of genes from all of the major repair pathways. As a means of providing context to the activity of these genes, the following section will briefly summarize each of the major DNA repair pathways in mammals (incidentally, these pathways are largely conserved between organisms as evolutionarily distant from mammals as bacteria and yeast [76]).

1.6.1 Overview of Major DNA Repair Pathways in Mammals

1.6.1.1 Base Excision Repair

The Base Excision Repair (BER) pathway removes bases that have been damaged by alkylation, oxidation, deamination or depurination/depyrimidination, and fills the resulting gap with non-damaged nucleotides [77]. Bases that have undergone alteration in the form of alkylation, oxidation or deamination may interfere with correct Watson-Crick base-pairing during DNA replication and cause mutations to arise [78]. BER may also be involved in repair of single stranded breaks in DNA [79].

BER is initiated by recognition and cleavage of a damaged base by a DNA glycosylase. Various DNA glycosylases exist; certain enzymes may recognize bases damaged by oxidation while others recognize alkylated bases or mispaired uracil and thymine [77, 79, 80]. Cleavage of the N-glycosidic bond between the damaged base and the attached sugar molecule creates an abasic site, also called an AP site, which is subsequently removed completely from the DNA molecule following cleavage of the DNA backbone on either side of the damage site (in the repair of oxidative damage, cleavage of the DNA backbone and excision of the damaged base are simultaneous [79]) [77]. Once a DNA Polymerase has filled the abasic site with an undamaged nucleotide, ligase enzymes catalyze the formation of new bonds in the DNA backbone to seal the gap [77]. An alternative version of BER exists, called 'long patch repair', involving different DNA Polymerases, which synthesize a strand of 2 to 10 nucleotides at the site of the removed base [81]. Synthesis of the new strand causes displacement of the original error-containing DNA strand, which is subsequently removed.

Much of the damage repaired by BER is produced endogenously, due to reactive oxygen species and metabolic byproducts as opposed to external genotoxic agents. Accordingly, BER has been shown to be specifically important during early embryogenesis in mice, when embryos are shielded from exposure to many external sources of DNA damage [82].

The study of targeted mutations in DNA glycosylases have shown a high degree of functional redundancy [77, 83]. However, when multiple DNA glycosylases are targeted for mutation in mice, the lesions normally repaired by the DNA glycosylases accumulate, genomic instability ensues and mice are predisposed to develop tumors [83, 84]. By contrast, null mutations in enzymes participating in the post-glycosylase steps of BER result in embryonic lethality, making it difficult to study their effect on genome stability [77]. In humans, germline mutations in two BER genes have each been associated with predisposition to certain subtypes of colorectal cancer [85].

1.6.1.2 Nucleotide Excision Repair

Nucleotide Excision Repair (NER) is responsible for removing bulky lesions from DNA, including cyclopyrimidine dimers and 6-4 photoproducts[86-88]. The types of lesions repaired by NER cause thermodynamic instability within the DNA double-helix structure and interfere with DNA replication and transcription [87]. Two main forms of NER have been described, reviewed in [89]: (i) transcription-coupled repair, which recognizes bulky lesions when an RNA Polymerase enzyme stalls during transcription of an active gene; (ii) global genomic repair, which does not rely on RNA Polymerase for damage recognition, and may therefore detect helix-distorting lesions throughout the genome, regardless of transcriptional status. While the initial recognition of damage involves different enzymes in transcription-coupled versus global genomic repair, the rest of the NER process is the same across both sub-pathways. In brief, a short stretch of nucleotides containing the lesion is excised from the affected strand and DNA Polymerase uses the complementary strand as a template to synthesize a replacement stretch of nucleotides to fill the resulting gap [90].

Many of the lesions recognized and repaired by the NER pathway are caused by exposure to ultraviolet radiation and environmental mutagens, however, more recently, several studies have also implicated NER in repair of oxidative damage, alongside BER[91]. It was noted that patients suffering from NER deficiencies were not only predisposed to skin cancer but also developed phenotypes in tissues shielded from ultraviolet radiation, therefore implying a broader repair role for the NER pathway. In this context, it is conceivable that NER may represent an important repair mechanism in the developing embryo, despite limited exposure of the mammalian embryo to ultraviolet light or other exogenous insults. Indeed, there have been several studies demonstrating that NER constitutes part of the repair apparatus in mouse embryonic stem cells [92, 93]. Furthermore, knockout mutations in a gene encoding a component to a complex central to NER cause complete NER deficiency and embryonic lethality in mice [94].

Congenital mutations in global genomic NER genes result in xeroderma pigmentosum, a disease associated with an increased risk of skin cancer greater than 1000-fold, due to

deficient repair of ultraviolet-induced lesions in sun-exposed skin [95, 96]. In addition, severe forms of this disease result in a various brain tumors and progressive neuron death due to accumulated oxidative damage [91, 96]. It was found that mice with targeted mutations in global genomic NER genes develop internal tumors in addition to skin cancers, after treatment with chemical carcinogens [97].

1.6.1.3 Homologous Recombination and Non-Homologous End Joining

Homologous Recombination (HR) and Non-Homologous End Joining (NHEJ) are responsible for repair of double-stranded breaks (DSBs) in DNA. DSBs are often cited as the lesions with the largest potential for deleterious downstream consequences, as they are believed to trigger apoptosis more readily than other forms of DNA damage [98], and repair of these lesions is complex and, at times, error-prone [99]. DSBs arise largely as a result of radiation- or chemical-induced damage, but can also be caused by endogenous sources, such as byproducts of cellular metabolism [99, 100]. Additionally, the DNA replication forks may collapse when replication machinery encounters a single stranded break or other DNA lesion, and this collapse may give rise to a DSB [99].

Of the two DSB repair pathways, NHEJ is the most error-prone, as it does not rely on a homologous DNA sequence for repair and can result in loss of genetic material and occasionally, chromosomal translocations [100]. At the site of a DSB, heterodimeric proteins bind to the double-stranded ends of the DNA on either side of the break and recruit DNA-dependent protein kinases. DNA ligases are eventually recruited to directly join the two double-stranded ends back together, reviewed in [101]. In some instances, the DNA on either side of the DSB is degraded by exonucleases prior to ligation [99].

The initial step of HR is always recruitment of exonucleases to the site of a DSB to trim the ends of the DNA and produce long single-stranded tails protruding at the 3’ ends. The exposed 3’ ends can then invade the double-stranded helix structure of a homologous segment of DNA (for example, on a homologous chromosome or sister chromatid), and use the homologous sequence as a template to synthesize new DNA over the DSB region. The 3’ ends act as primers for the synthesis of new DNA. These steps are reviewed in [101].

A study comparing expression of HR and NHEJ enzymes in mouse embryos found that embryonic stem cells (progenitor cells that must give rise to many different cell types in the mature organism), preferentially repair DSBs with the HR pathway rather than the error-prone NHEJ pathway[102, 103]. Conversely, NHEJ is favored in the differentiated embryonic cells and adult mammalian cells, although HR is still operational and may complement NHEJ repair [102-104].

Famously, mutations in the DSB-repair genes *BRCA1* and *BRCA2* are associated with predisposition to breast and ovarian cancers, and research into the association between these genes and cancer risk has helped broaden the understanding of the HR pathway [105-107]. Several other HR genes have been implicated in human cancers, including associations between mutations in *RAD54B* and colon cancer [108].

Targeted mutations in mouse NHEJ genes have been shown to cause embryonic lethality in some cases [109], and cancer-susceptibility in others [109]. In humans, however, inactivating mutations in NHEJ genes are very rarely found [110]. A small number of NHEJ mutations have been described in radiosensitive cancer patients; these are believed to alter the expression or efficiency of NHEJ enzymes, without abolishing their activity completely [111, 112].

1.6.1.4 Mismatch Repair

Mismatch Repair (MMR) genes were first described in studies of bacteria and yeast cell lines with high spontaneous mutation rates [113-115]. Since then, homologues have been identified in humans, mutations in which are associated with mutator phenotypes and cancer predisposition [116, 117]. MMR is responsible for recognizing and removing base-pair mismatches that have occurred as the result of recombination, small insertions or deletions in the genome, or erroneous polymerization during DNA replication. Once a mismatch has been detected, it is important that MMR machinery is able to distinguish between the parental strand of DNA, containing the original genetic code, and (in the case of post-replication MMR), the newly-synthesized daughter strand, containing the incorrect base. Following detection of the mismatch and identification of the daughter strand, an exonuclease is recruited which degrades a portion of the DNA strand

containing the mismatch. The missing portion of the daughter strand can then be polymerized and ligated, reviewed in [118].

Mutations in several genes within the MMR pathway have been linked to Lynch Syndrome, an inherited condition associated with increased risk of colon cancer, endometrial cancer, and several other extra-colonic cancers [119]. Notably, a recent study by Ahadova et al. linked MMR-deficient foci in the intestines of Lynch syndrome patients with activating mutations in the *CTNNB1* gene (within the same exon, exon 3, as is affected in *CTNNB1*-mutant Wilms tumors) [5]. Another study found that activating mutations in exon 3 of *CTNNB1* are associated specifically with MMR-deficient melanomas, compared to MMR-proficient melanoma cell lines; this provides an example of deficient DNA repair and constitutive WNT/beta-catenin signaling cooperating in oncogenesis [6].

In addition to studies in human cancer patients with mismatch deficiencies, mouse models have been created to study the effect of both constitutive and conditional inactivation of MMR genes [120]. Especially with conditional MMR mutation systems, the cancer predisposition phenotype observed in mice closely mimics what is seen in humans. Interestingly, several studies in mice have suggested a role for MMR components in other DNA repair pathways, including NER of UV-induced damage [121] and BER of oxidative lesions [122].

1.6.2 Associations between Wilms Tumor and DNA Repair Deficiencies in Literature

As discussed above, there are numerous associations between increased risk of various cancers and mutations in DNA repair genes, (also concisely reviewed in [4]). However, few studies have examined DNA repair in the context of Wilms tumor specifically. In 2005, Reid et al. described a number of children with constitutional biallelic mutations in the DNA repair gene *BRCA2* who developed multiple cancers in childhood, including Wilms tumors [123]. A subset of Wilms tumor cases have been described with mutations in *TP53* [124], a gene which helps direct excision-based DNA repair (in addition to cell cycle arrest and apoptosis), as a response to genomic damage [125]. *WT1* mutations were

not detected in any of the Wilms tumors with *TP53* mutations discussed in [124]. The authors state that their study does not provide sufficient evidence of mutual exclusivity between *WT1* and *TP53* mutation. However, if, as we propose, *WT1* mutations and *TP53* mutations result in the same downstream consequence of compromised DNA repair, we would not expect *WT1* and *TP53* mutations to occur within the same Wilms tumor. It is not explicitly stated in [123], whether the Wilms tumors from patients with constitutional *BRCA2* mutations also carry mutations in *WT1*. It would be of great interest to determine whether similar activating mutations in the beta-catenin/WNT signaling pathway are observed in the rare subset of Wilms tumors harbouring mutations in *TP53* or *BRCA2*.

In 2013, Diniz and coworkers tried to establish a link between Wilms tumor, deficiency in proteins within the MMR pathway, and microsatellite instability (MSI) [126]. MSI is caused by unrepaired erroneous replication of small, highly repetitive segments of DNA (microsatellites), leading to changes in microsatellite length. MSI is considered a marker of MMR deficiency and is observed in almost all patients with Hereditary Non Polyposis Colon Cancer [127]. Although a clear link between germline mutations in genes encoding MMR proteins and MSI-positive Hereditary Non Polyposis Colon Cancer had been previously established [128], Diniz et al. were interested in exploring a role for deficient MMR and MSI in other malignancies; namely, Wilms tumor [126]. Using immunohistochemistry, Diniz found that 19 of the 45 Wilms tumors examined showed loss of expression of key MMR proteins. MSI was found in very few of the tumors, and only to a limited extent. Conversely, loss of MMR protein expression correlated well with both the stage of the disease and survival rate, and authors suspected that germline mutations in MMR genes were a contributing factor in nearly half the Wilms tumor cases studied [126]. In this thesis, we will present why we believe deficiencies in DNA repair, perhaps including the MMR pathway, might be implicated in Wilms tumorigenesis.

1.7 Research Proposal

The hypothesis for this project is two-fold. Firstly, we hypothesize that there is a panel of DNA repair genes activated in the NPCs of the embryonic kidney, accompanying the proliferative burst required for kidney formation. The second

component of our hypothesis is that a subset of these DNA repair genes are WT1-dependant, and thus WT1 is critical for protecting NPCs from acquiring oncogenic mutations.

Objective 1A: identify a panel of DNA repair genes expressed at a higher level in the embryonic compared to the adult mouse kidney. To do this, we took an open-ended approach and used a pathway-focused Reverse Transcription quantitative Polymerase Chain Reaction (RT-qPCR) Array that quantified the expression of 84 DNA repair genes in the embryonic and adult kidneys of wildtype mice.

Objective 1B: further localize the expression of certain DNA repair genes within the embryonic kidney, and determine whether the expression of any of these genes is enriched in the NPCs (the cells which may give rise to Wilms tumors), relative to total kidney. To test this, we used a mouse model where a fluorescent red protein is expressed selectively in *Cited1(+)* cells of the embryonic kidney, representing the NPCs within the CM. Fluorescence-Activated Cell Sorting (FACS) was then used to isolate *Cited1(+)* NPCs from total kidney cell pools. With RT-qPCR, we compared expression of DNA repair genes in *Cited1(+)* cells to that of total kidney cell pools. We were also interested in quantifying expression of DNA repair genes within a second, also rapidly-dividing, embryonic kidney compartment. For this, we used a transgenic mouse which expresses a green fluorescent protein specifically within the *Hoxb7*(+) cells, representing the UB cells and their derivatives. We used FACS followed by RT-qPCR to compare the expression of DNA repair genes in *Hoxb7(+)* cells relative to total kidney cell pools from littermates. Our plan was to identify a subset of DNA repair genes enriched in the *Cited1(+)* cells of the embryonic kidney specifically.

Objective 2: ascertain whether the expression of certain DNA repair genes is WT1-dependent. We used RT-qPCR to assess whether the expression of DNA repair genes was reduced following the conditional knockout of *Wt1*, specifically from FACS-isolated nephron progenitors in mice.

CHAPTER 2: MATERIALS AND METHODS

2.1 Breeding, Timing of Litters, and Handling of Mice

Female mice were weighed on the first day of mating so that subsequent weight gain could be monitored and used to determine pregnancy status. To maximize chance of pregnancy, mating pairs or trios (two females of the same genotype and one male), were kept in the same cage for a maximum of three consecutive nights, after which the male was removed. If no vaginal plug was observed in a female that became pregnant, the day following the first night with the male was taken as day 0.5 post-coitus. Dissections of embryos were scheduled for E17.5 of development, which is very close to the full gestational period in C57BL/6J, therefore the earliest possible conception date was assumed (when no vaginal plug was visible), so as to minimize risk of birth precluding the dissection of embryos.

All mice were maintained on a C57BL/6J genetic background, apart from the *Hoxb7*^{GFP} mice, which are CD-1. All mice were handled in accordance with the guidelines of the Canadian Council on Animal Care and the McGill University Animal Care Committee.

2.2 Microdissection of E17.5 Kidneys from C57BL/6J Wildtype Mice for RT-qPCR Array

Pregnant dams (N=3) were sacrificed when the embryos had matured to E17.5. Embryos were rinsed in PBS (Corning, cat. # 21-040-CV) and kept on ice up until the moment of dissection. A dissecting microscope (Leica MZ75) and dissecting forceps were used to remove embryonic kidneys. The kidney pairs from all embryos within a litter were pooled into a single tube, rinsed in PBS (Corning), and placed at -80° C. On average, there were 8.7 embryos per litter.

2.3 Kidney Harvest from Adult C57BL/6J Wildtype Mice for RT-qPCR Array

Kidneys from 3 adult male C57BL/6J wildtype mice (4 months of age), were removed using dissecting forceps and cut into small chunks, roughly 3 mm^3, using a straight blade. Kidney chunks were frozen at -80° C.

2.4 Total RNA Extraction from E17.5 and Adult Kidneys of C57BL/6J Wildtype Mice for RT-qPCR Array

Total RNA was extracted from each pool (N=3) of E17.5 kidneys and from adult C57BL/6J wildtype kidney tissue (N=3) using the EZ-10 DNAaway RNA Miniprep Kit (Bio Basic, cat. # BS88133). Following kit specifications, 30 milligrams of frozen kidney tissue was used in each reaction. RNA was eluted in 30 μL of nuclease-free water and the quality and concentration of the RNA in each sample was determined by spectrophotometry.

2.5 DNA Repair-Focused RT-qPCR Array

RNA extracted from adult and embryonic C57BL/6J wildtype kidneys was reverse transcribed into cDNA, using the RT^2 First Strand Kit (Qiagen, cat. # 330401). 500 ng of RNA was added into each reverse transcription reaction. Each sample was incubated with a genomic DNA elimination buffer at 42°C for 5 minutes, and then placed on ice. A reverse transcription mix, containing RE3 Reverse Transcriptase enzymes, was added to each sample and the samples were incubated at 42°C for 15 minutes, then at 95°C for 5 minutes.

To quantify the expression of DNA repair genes in the cDNA samples prepared with the RT^2 First Strand Kit, a PCR components mix was made for each cDNA sample, using RT^2 SYBR Green Mastermix (Qiagen, cat. # 330502). Each PCR components mix contained 1350 μL of RT^2 SYBR Green Mastermix solution, 102 μL of the cDNA synthesis reaction, and 1248 μL of RNase-free water. 25 μL of each PCR components mix was loaded into each well of a 96-well DNA-repair-focused RT^2 Profiler PCR Array (Qiagen, cat. # PAMM-042ZF-12). The DNA-repair-focused RT^2 Profiler PCR Array contains verified primer sets that target 84 DNA repair genes across multiple repair pathways, as well as primers to amplify 6 common housekeeping genes and various positive and negative controls. qPCR was performed on a LightCycler 480 Instrument II (Roche, product # 05015278001), with the following cycling conditions: 10 minutes at 95°C, followed by 45 cycles of 15 seconds at 95°C and 1 minute at

60°C. The threshold cycle (C_T) was calculated for each well using the second derivative max setting of the LightCylcer 480 software.

2.6 Genotyping of *Cited1*$^{CreER(T2)}$, *R26*^{tdTomato}, *Wt1*^{flox} and *Hoxb7*^{GFP} Mice

When genotyping mice for further breeding or colony maintenance, tail biopsies were collected from mice at age 21 days, upon weaning of pups from their mothers. For genotyping embryos, the tail of each embryo was removed upon dissection at E17.5. Genomic DNA from tails was extracted and amplified by PCR using the Sigma Extract-N-Amp Tissue PCR kit (Sigma, product # XNAT2). PCR reaction mix included in the kit was used with primers specific for: (i) *Cited1*$^{CreER(T2)}$ or the wildtype *Cited1*$^{+}$; (ii) *R26*^{tdTomato} or the wildtype *R26*$^{+}$; (iii) *Wt1*^{flox} or the wildtype *Wt1*$^{+}$; or (iv) *Hoxb7*^{GFP}. Each PCR reaction contained 10 μL of PCR Reaction Mix, 0.2 μM final concentration of each primer, 4 μL of genomic DNA and distilled water up to a total reaction volume of 20 μL.

2.6.1 *Cited1*$^{CreER(T2)}$ and *Cited1*$^{+}$ Mice: Description of Mouse Strain, Genotyping Primers, PCR Cycling Conditions

Cited1$^{CreER(T2)}$ mice, initially genetically engineered by Boyle et al. [18], express a tamoxifen-inducible Cre recombinase gene under control of the BAC *Cited1* promoter. Boyle et al. have previously shown that expression of the BAC transgene closely replicates endogenous CITED1 protein expression [18]. The primers used to amplify the wildtype *Cited1* locus for genotyping were: Forward 5' TTA CTT GCA GAC CAA CAG GC 3' and Reverse 5' TGC TTC TTT GAC CCA TTT CC 3'. The primers used to amplify the *Cited1*$^{CreER(T2)}$ transgene insertion were: Forward 5' TCC AAT TTA CTG ACG GTA CAC CAA 3' and Reverse 5' CCT GAT CCT GGC AAT TTC GGC TA 3'.This *Cited1*$^{CreER(T2)}$ mouse strain was donated to our lab by Mark de Caestecker and colleagues.

The thermal cycling conditions for the *Cited1* program were: 95°C for 3 minutes, followed by 36 cycles of 30 seconds at 94°C, 30 seconds of 58°C and 30 seconds of 72°C, followed by 3 minutes at 72°C and holding the samples finally for an indefinite period at 4°C.

PCR products were electrophoresed on a 2% agarose gel, containing Ethidium Bromide, for 20 minutes at 100 V. Mice containing the *Cited1*$^{CreER(T2)}$ transgene insertion displayed a band at 540 bp. Mice wildtype at the *Cited1* locus displayed a band at 367 bp. Figure 2A shows a representative gel electrophoresis image of the bands produced by mice containing the *Cited1*$^{CreER(T2)}$ transgene insertion versus mice with no insertion (*Cited1*$^{+/+}$).

2.6.2 *R26*^{tdTomato} and *R26*$^{+}$ Mice: Description of Mouse Strain, Genotyping Primers, PCR Cycling Conditions

R26^{tdTomato} mice were obtained from The Jackson Laboratory. This reporter strain harbors a Rosa-CAG-LSL-tdTomato-WPRE::deltaNeo construct inserted into the Gt(ROSA)26Sor locus (*R26)*. This construct consists of a gene encoding a fluorescent red reporter protein (tdTomato), driven under a strong, constitutive, synthetic promoter. The *tdTomato* gene contains a stop cassette flanked by loxP sites, allowing excision of the stop codon and expression of tdTomato only in cells where Cre recombinase is expressed. The primers used to amplify the wildtype *R26* locus for genotyping were: Forward 5' AAG GGA GCT GCA GTG GAG TA 3'and Reverse 5' CCG AAA ATC TGT GGG AAG TC 3'. The primers used to amplify the Rosa-CAG-LSL-tdTomato-WPRE::deltaNeo construct were: Forward 5' CTG TTC CTG TAC GGC ATG G 3' and Reverse 5' GGC ATT AAA GCA GCG TAT CC 3'.

The thermal cycling conditions for the *R26* program were: 94°C for 3 minutes, followed by 35 cycles of 20 seconds at 94°C, 30 seconds of 61°C and 30 seconds of 72°C, followed by 2 minutes at 72°C and holding the samples finally for an indefinite period at 10°C.

PCR products were electrophoresed on a 2% agarose gel, containing Ethidium Bromide, for 20 minutes at 100 V. Mice containing the Rosa-CAG-LSL-tdTomato-WPRE::deltaNeo construct displayed one band at 196 bp. Mice wildtype at the *R26* locus displayed one band at 297 bp. Figure 2B shows a representative gel

electrophoresis image of the bands produced by mice containing the Rosa-CAG-LSL-tdTomato-WPRE::deltaNeo construct versus mice wildtype at the *R26* locus.

2.6.3 *Wt1*^{flox} and *Wt1*$^{+}$ Mice: Description of Mouse Strain, Genotyping Primers, PCR Cycling Conditions

The *Wt1* conditional knockout mouse strain (*Wt1*$^{flox/flox}$) was generated by Gao et al. in 2006[129]. Breeding pairs of *Wt1*$^{flox/flox}$ mice were purchased from The Jackson Laboratory. Both *Wt1* alleles in *Wt1*$^{flox/flox}$ mice have loxP sites flanking exons 8 and 9 of the *Wt1* gene (exons 8 and 9 are 'floxed'). Upon expression of Cre recombinase, exons 8 and 9 are excised from the gene and the resultant WT1 protein, which lacks 2 of the 4 WT1 zinc fingers, is non-functional. Gao et al. have previously shown that expression of Cre recombinase from the earliest stages of embryogenesis caused death of *Wt1*$^{flox/flox}$ mouse embryos at the same time point as *Wt1*-/- embryos [129], (which contain constitutive targeted mutations of the *Wt1* gene [29]). Importantly, ablation of just one *Wt1* allele (in *Wt1*$^{flox/+}$ mice, for example), results in a wildtype phenotype and viable mice. The same primers were used to amplify both the loxP-flanked *Wt1* allele and wildtype *Wt1*: Forward 5' TGG GTT CCA ACC GTA CCA AAG 3' and Reverse 5' GGG CTT ATC TCC TCC CAT G'.

The thermal cycling conditions for the *Wt1* program were: 94°C for 2 minutes, followed by 35 cycles of 15 seconds at 94°C, 30 seconds of 58°C and 1 minute of 72°C, followed by 5 minutes at 72°C and holding the samples finally for an indefinite period at 4°C.

PCR products were electrophoresed on a 2% agarose gel, containing Ethidium Bromide, for 20 minutes at 100 V. Mice containing two floxed copies of the *Wt1* allele displayed a single band at 230 bp. Mice containing two wildtype *Wt1* alleles displayed a single band at 196 bp. Mice heterozygous for the floxed *Wt1* allele displayed two bands, one at 230 bp and another at 196 bp. Figure 2C shows a representative gel electrophoresis image of the bands produced by mice homozygous for the floxed *Wt1* allele versus mice heterozygous at this locus.

2.6.4 *Hoxb7*^{GFP} Mice: Description of Mouse Strain, Genotyping Primers, PCR Cycling Conditions

The generation of *Hoxb7*^{GFP} mice was described by Srinivas et al. in 1999 [130]. These mice express a green fluorescent protein (GFP) under control of the *Hoxb7* promoter, which drives expression specifically in the nephric duct and UB cells of the developing kidney, and their epithelial derivatives in the mature structure. The primers used to amplify the *Hoxb7*^{GFP} transgene for genotyping were: Forward 5' AGC GCG ATC ACA TGG TCC TG 3' and Reverse 5' ACG ATC CTG AGA CTT CCA CAC T 3'. The wildtype *Hoxb7* promoter was not amplified in this genotyping process. *Hoxb7*^{GFP} mice were donated to the Paul Goodyer laboratory by Dr. Indra Gupta at McGill University.

The thermal cycling conditions for the *Hoxb7*^{GFP} program were: 94°C for 1 minutes, followed by 30 cycles of 30 seconds at 94°C, 30 seconds of 62°C and 30 seconds of 72°C, followed by 7 minutes at 72°C and holding the samples finally for an indefinite period at 16°C.

PCR products were electrophoresed on a 2% agarose gel, containing Ethidium Bromide, for 20 minutes at 100 V. Mice containing the *Hoxb7*^{GFP} transgene insertion displayed one band at 321 bp. Mice wildtype at the *Hoxb7* locus did not display any band. Figure 2D shows a representative gel electrophoresis image of the bands produced by mice containing the *Hoxb7*^{GFP} insertion and the absence of bands in mice lacking the insertion.

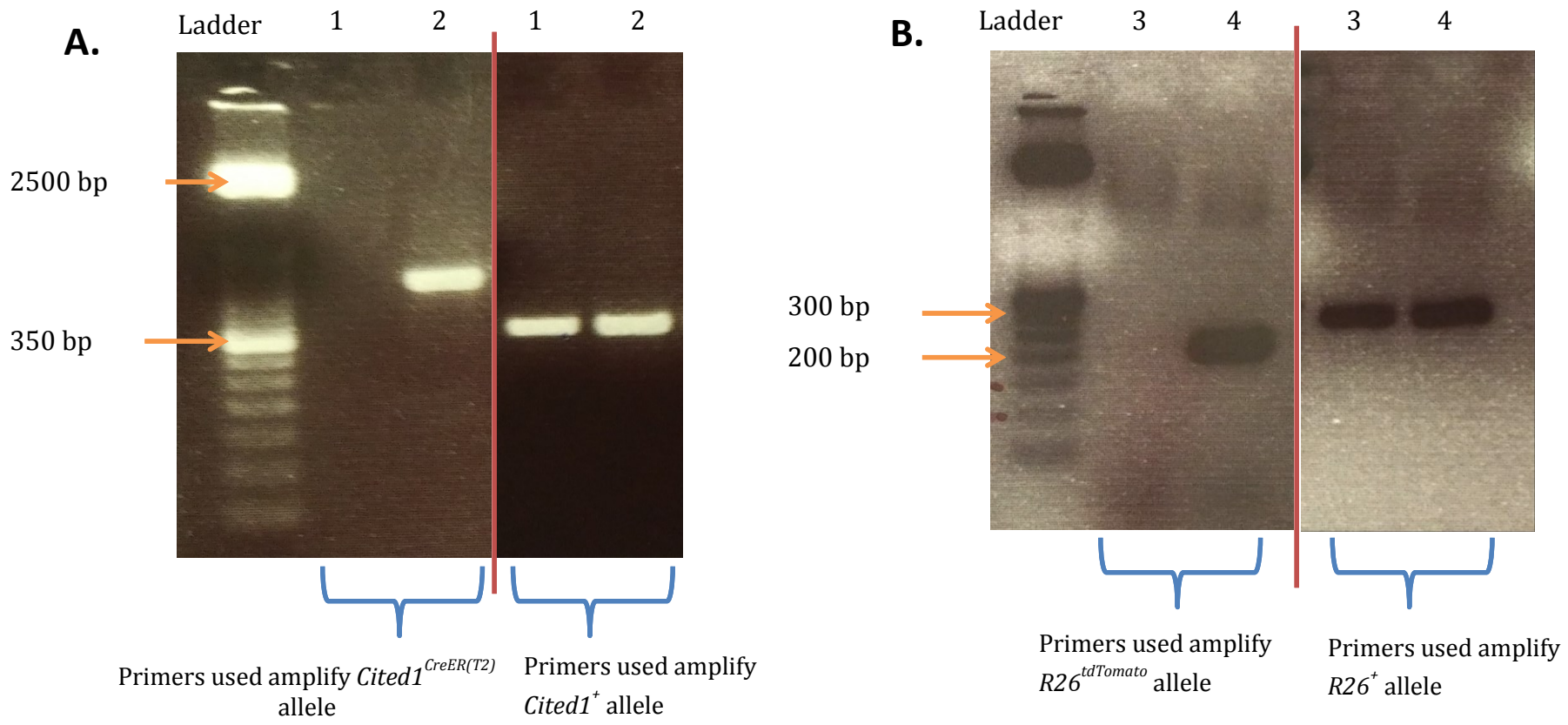

Figure 2. Representative mouse genotyping images using gel electrophoresis and PCR primers that amplify *Cited1*$^{CreER(T2)}$ or *Cited1*$^{+}$ alleles (A), the *R26*^{tdTomato} or *R26*$^{+}$ alleles (B), the *Wt1*^{flox} or *Wt1*$^{+}$ alleles (C) and the *Hoxb7*^{GFP} allele (D).

All samples run on 2% agarose gels stained with Ethidium bromide. In (A), Sample 1 is from a mouse with the genotype *Cited1*$^{+/+}$ and Sample 2 is from a mouse with the genotype *Cited1*$^{CreER(T2)/+}$. In (B), Sample 3 has the genotype *R26*$^{+/+}$ and Sample 4 has the genotype *R26*$^{tdTomato/+}$. In (C), Sample 5 has the genotype *Wt1*$^{flox/flox}$ and Sample 6 has the genotype *Wt1*$^{flox/+}$. In (D), Sample 7 is from a mouse that is wildtype at the *Hoxb7* locus (*Hoxb7*$^{+/+}$) and Sample 8 is from a mouse with the genotype *Hoxb7*^{GFP}.

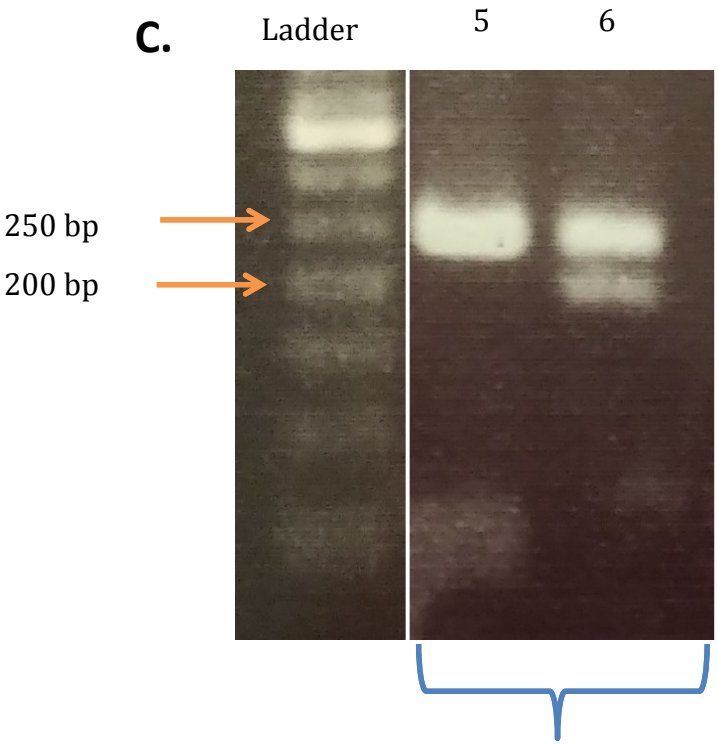
C.
Ladder
5
6
250 bp
200 bp
Primers used amplify both
Wt1+ and Wt1flox alleles

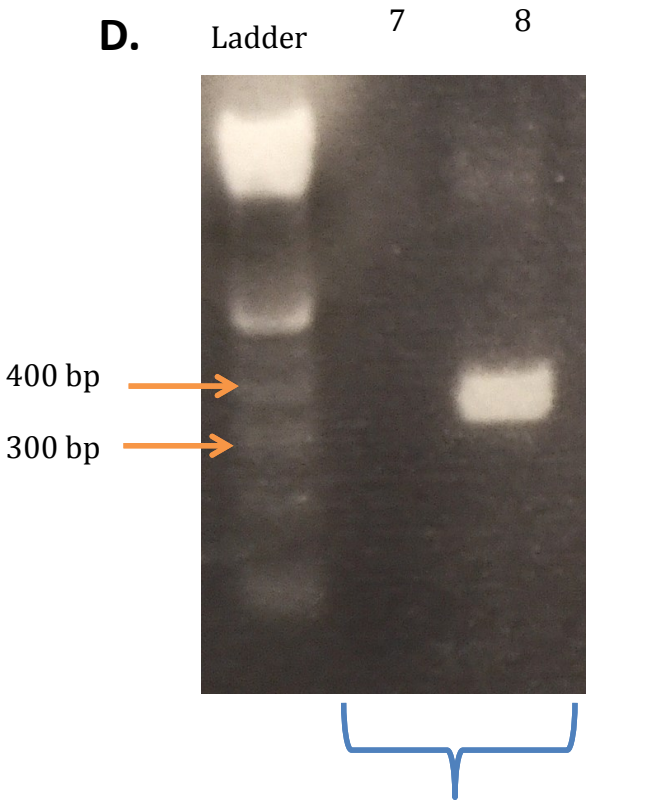
D.
Ladder
7
8
400 bp
300 bp
Primers used amplify the
Hoxb7GFP allele

2.7 Breeding Schemes

2.7.1 Breeding Scheme for *Cited1*$^{CreER(T2)/+}$; *R26*$^{tdTomato/+}$ Mice

Cited1$^{CreER(T2)/+}$ mice were mated with mice homozygous for the *tdTomato* insert at the *R26* locus (*R26*$^{tdTomato/tdTomato}$). Approximately half of the resultant embryos had the *Cited1*$^{CreER(T2)}$ transgene insertion and all embryos were heterozygous at the *R26* locus (*Cited1*$^{CreER(T2)/+}$; *R26*$^{tdTomato/+}$). Figure 3 depicts the breeding scheme to produce *Cited1*$^{CreER(T2)/+}$; *R26*$^{tdTomato/+}$ embryos.

2.7.2 Breeding Scheme for *Cited1*$^{CreER(T2)/+}$; *R26*$^{tdTomato/+}$; *Wt1*$^{flox/flox}$ Mice

Cited1$^{CreER(T2)/+}$ mice were mated with *Wt1*$^{flox/flox}$ mice. The *Cited1*$^{CreER(T2)/+}$;*Wt1*$^{flox/+}$ pups from the resultant litter were backcrossed to the *Wt1*$^{flox/flox}$ strain until *Cited1*$^{CreER(T2)/+}$;*Wt1*$^{flox/flox}$ mice were obtained. In parallel, *Wt1*$^{flox/flox}$ mice were crossed with the *R26*$^{tdTomato/tdTomato}$ strain to produce *R26*$^{tdTomato/+}$; *Wt1*$^{flox/+}$ pups. These pups were self-crossed until *R26*$^{tdTomato/tdTomato}$; *Wt1*$^{flox/flox}$ mice were obtained. Finally, *R26*$^{tdTomato/tdTomato}$; *Wt1*$^{flox/flox}$ mice were crossed with *Cited1*$^{CreER(T2)/+}$;*Wt1*$^{flox/flox}$ mice and approximately half of the resultant embryos had the genotype *Cited1*$^{CreER(T2)/+}$; *R26*$^{tdTomato/+}$; *Wt1*$^{flox/flox}$. Figure 4 depicts the breeding scheme to produce *Cited1*$^{CreER(T2)/+}$; *R26*$^{tdTomato/+}$; *Wt1*$^{flox/flox}$ embryos.

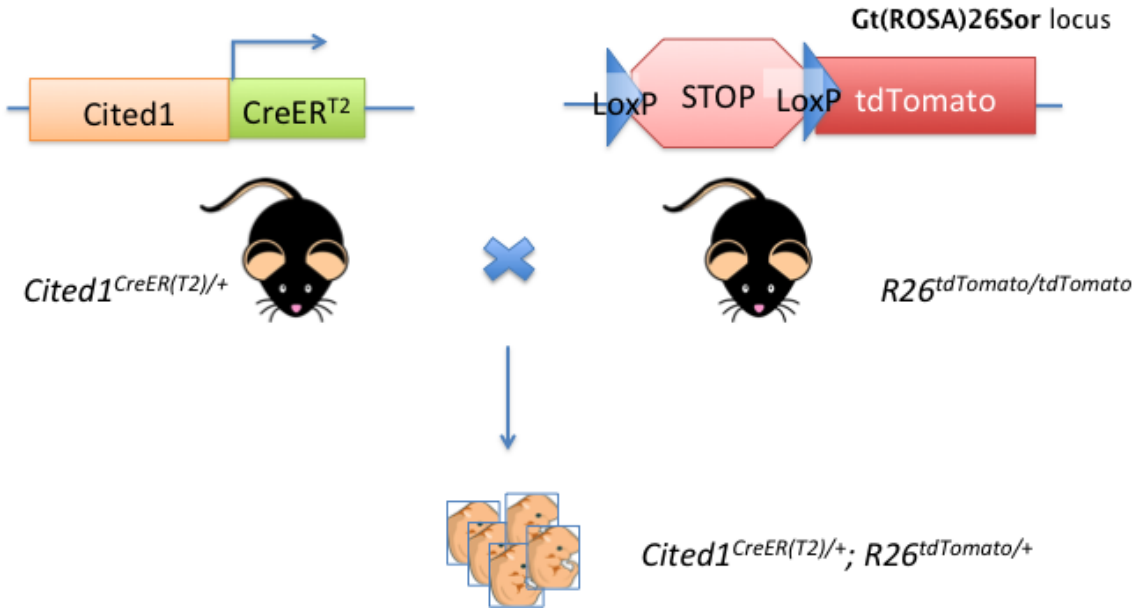

Figure 3. Breeding scheme used to produce *Cited1$^{CreER(T2)/+}$; R26$^{tdTomato/+}$* embryos.

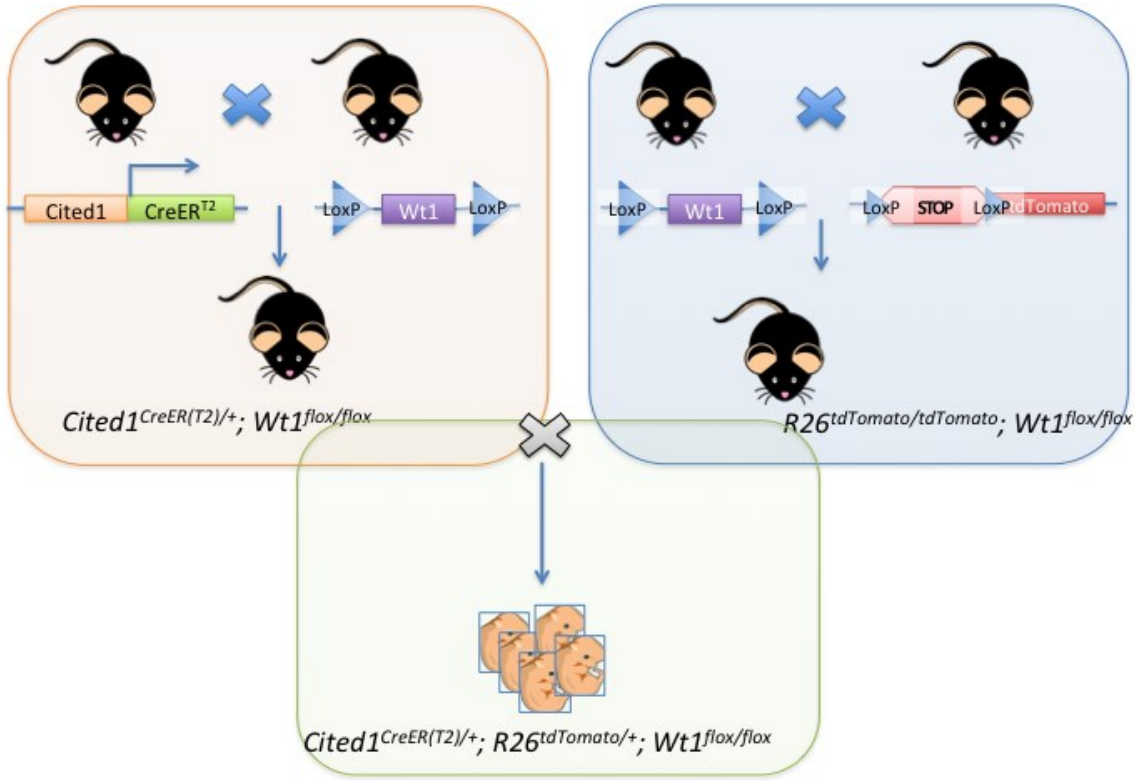

Figure 4. Breeding scheme to produce *Cited1$^{CreER(T2)/+}$; R26$^{tdTomato/+}$; Wt1$^{flox/flox}$* embryos.

2.8 Microdissection of Embryonic Kidneys from *Cited1*$^{CreER(T2)/+}$; *R26*$^{tdTomato/+}$, *Cited1*$^{CreER(T2)/+}$; *R26*$^{tdTomato/+}$; *Wt1*$^{flox/flox}$ and *Hoxb7*^{GFP} Mouse Embryos

Pregnant dams were sacrificed when the embryos had matured to E17.5. Embryos were rinsed in PBS (Corning) and kept on ice up until the moment of dissection. A dissecting microscope (Leica MZ75) and dissecting forceps were used to remove embryonic kidneys. Embryos were each assigned a letter in order of dissection (Embryo A, B, C, for example), and the kidney pair of each embryo was placed in a correspondingly labeled tube and rinsed with PBS (Corning). At the point of dissection, the tail of each embryo was removed and placed in an empty, labeled tube for genotyping by PCR (genotyping procedures previously described).

2.9 Mechanical and Chemical Dissociation of Embryonic Kidneys and Monolayer Culture of Cells

Each embryonic kidney pair was incubated at 37°C, 5% CO_2 for 45 minutes in 1 mL of digesting solution until solution could be homogenized by gently pipetting up and down. Digestion solution contained 1 mg/mL Collagenase B (Roche, cat. # 11088807001), 2.5 mg/mL Dispase II (Roche, cat. # 04942078001), 2% FBS (Wisent, product # 080-450) and 1 Unit/mL DNase I (Roche Diagnostics, product # 118286650) in PBS (Corning). Tubes containing dissociated embryonic kidney cells in digest solution were centrifuged at 1000 rpm for 5 minutes and the supernatant was decanted. Cell pellets were resuspended in 5 mL of cell culture medium containing 1X ITS (Corning, cat. # MT25800CR), DMEM (Corning, cat. # MT10013CV), 10% FBS (Wisent), and 1% Penicilin-Streptyomycin (Gibco, cat. # 15140122), then transferred to a sterile cell culture flask. Flasks, each labeled with the embryo identification letter, were incubated at 37°C, 5% CO_2 for 24 hours, before treatment with (Z)-4-Hydroxy Tamoxifen (4OHT).

2.10 Activation of Fluorescence in *Cited1*$^{CreER(T2)/+}$;*R26*$^{tdTomato/+}$ and *Cited1*$^{CreER(T2)/+}$;*R26*$^{tdTomato/+}$;*Wt1*$^{flox/flox}$ mice by *in vitro* Treatment of Embryonic Kidney Cells with (Z)-4-Hydroxy Tamoxifen (*Hoxb7*^{GFP} Embryonic Kidney Cells also Treated)

All media was aspirated from culture flasks containing dissociated embryonic kidney cells, and replaced with media containing 4OHT (Toronto Research Chemicals, cat. # H954725) in a 0.0025 mg/mL concentration. This concentration of 4OHT was previously determined by a graduate student in our lab to be an

optimal concentration for activating fluorescence in dissociated embryonic kidney cells of *Cited1*$^{CreER(T2)/+}$;*R26*$^{tdTomato/+}$ mice. Culture flasks were then incubated with the 4OHT-containing media at 37°C, 5% CO_2 for 24 hours, after which time cells were trypsinized and collected for FACS analysis. Embryonic kidney monocultures from the *Hoxb7*^{GFP} lineage were also treated identically with 4OHT for consistency, although fluorescence in these cells is independent of 4OHT activation.

2.11 Isolation of Nephron Progenitor Cells from *Cited1*$^{CreER(T2)/+}$;*R26*$^{tdTomato/+}$ and *Cited1*$^{CreER(T2)/+}$;*R26*$^{tdTomato/+}$;*Wt1*$^{flox/flox}$ Embryonic Kidneys by Fluorescent Activated Cell Sorting

For each litter: cells were examined under a fluorescent microscope (Zeiss Axiovert 40 CFL) and flasks with visible red fluorescence were trypsinized for 5 minutes using 0.25% trypsin/EDTA (Corning, cat. # MT25053CI) and pooled into a single sample for FACS analysis. Flasks with no visible fluorescent cells were trypsinized for 5 minutes and combined into a single total kidney cell pool. All embryos were genotyped using PCR (method described previously) to confirm biochemically which embryos carried the *Cited1*$^{CreER(T2)}$ transgene insertion. Cells were washed with cell culture medium, and centrifuged at 1000 rpm for 5 minutes. The total kidney cell pool pellet was stored at -80°C until total RNA extraction. The FACS sample was resuspended in 0.5-1 mL of FACS media, containing 2% FBS (Wisent) in PBS (Corning), and filtered using a 70 μm cell strainer. Cells expressing the red fluorescent tdTomato protein represent the *Cited1*-expressing NPCs of the embryonic kidney and the structures derived from NPCs in the 24 hours since Cre activation. These red fluorescent cells were separated from the remainder of the cells in the sample during FACS. *Cited1(+)* cells collected during FACS were centrifuged at 12,000 rpm for 30 seconds and stored at -80°C until total RNA extraction.

2.12 Isolation of Ureteric Bud Cells from *Hoxb7*^{GFP} Embryonic Kidneys by Fluorescent Activated Cell Sorting

Monolayer cultures of cells from *Hoxb7*^{GFP} embryonic kidneys were examined under a fluorescent microscope (Zeiss Axiovert 40 CFL) and flasks with visible green fluorescence were trypsinized for 5 minutes (Corning, cat. # MT25053CI)

and pooled into a single sample for FACS analysis. Flasks with no visible fluorescent cells were trypsinized for 5 minutes and pooled into a single total kidney cell pool sample. Cells were washed with cell culture medium, and centrifuged at 1000 rpm for 5 minutes. The total kidney cell pool pellet was stored at -80°C until total RNA extraction. The FACS sample was resuspended in 0.5-1 mL of FACS media and filtered using a 70 μm cell strainer. Cells expressing GFP under the *Hoxb7* promoter represent the nephric duct, UB cells and their derivatives within the embryonic kidney. These green fluorescent cells were separated from the remainder of the cells in the sample during FACS. *Hoxb7(+)* cells collected during FACS were centrifuged at 12,000 rpm for 30 seconds and stored at -80°C until total RNA extraction.

2.13 Total RNA Extraction from Fluorescence-Sorted Cells and Total Kidney Cell Pools of Littermates

Cited1(+) cells from 4 litters of $Wt1^{+/+}$ mice were pooled into a single sample to provide a sufficient number of cells for total RNA extraction (approximately 490,000 cells in total). Similarly, *Cited1(+)* cells from 6 litters of $Wt1^{flox/flox}$ mice were pooled into a single sample of approximately 400,000 cells for total RNA extraction. *Hoxb7(+)* cells from 4 litters were pooled into a single sample of approximately 767,000 cells for RNA extraction.

RNA samples were prepared from 6 total kidney cell pools of $Wt1^{+/+}$ mice, 5 total kidney cell pools of $Wt1^{flox/flox}$ mice and 3 total kidney cell pools of $Hoxb7^{GFP}$ littermates. Total RNA was extracted from each sample using the Zymo Research Quick-RNA Microprep Kit (Zymo Research, cat. # R1050). The number of embryonic kidney pairs used in each reaction is included in Table 1, (designated by identification number of the pregnant dam). The microprep kit we used specifies that no more than 1 million cells should be used for each RNA extraction. As each individual total kidney cell pool consisted of many more than 1 million cells, we used ¼ of the pellet from each total kidney cell pool to extract RNA. In all cases, RNA was eluted in 15 μL of nuclease-free water and the quality and concentration of the RNA in each sample was determined by spectrophotometry.

Table 1. Composition of *Cited1(+)*, *Hoxb7(+)* and total kidney cell pool samples used for RNA extraction.

Table 1a.

Cited1(+) Cells Collected During FACS from *Cited1*$^{CreER(T2)/+}$;*R26*$^{tdTomato/+}$ Embryonic Kidneys		
Mouse ID # of Pregnant Dam	**# Embryonic Kidney Pairs Pooled into FACS Sample**	**# *Cited1(+)* Cells Collected During FACS**
208-5	6	93,902
215-1	4	81,000
215-2	4	105,000
208-2	7	211,000
Total # Cells used in RNA Extraction		**490,902**

Table 1b.

Total Kidney Cell Pools Collected from *Cited1*$^{+/+}$;*R26*$^{tdTomato/+}$ Embryos	
Mouse ID # of Pregnant Dam	**# Embryonic Kidney Pairs Pooled into Total Kidney Cell Pool Sample***
215-1	4
211-3	2
202-1	3
211-4	3
215-2	4
208-2	3
***1/4 of each total kidney cell pool pellet used in RNA extraction**	

Tables 1a, 1c, and 1e show the approximate number of *Cited1(+)* cells (1a, 1c) or *Hoxb7(+)* cells (1e) pooled into a single sample for RNA extraction, along with the number of embryonic kidney pairs included in each cell sorting experiment. Tables 1b, 1d, and 1f show the number of embryonic kidney pairs included in each cell pellet used for total kidney cell pool RNA extraction. For Tables 1b, 1d and 1f, each embryonic litter (designated by mouse ID number of pregnant dam) represents a separate RNA sample.

Table 1c.

Cited1(+) Cells Collected During FACS from *Cited1*$^{CreER(T2)/+}$;*R26*$^{tdTomato/+}$;*Wt1*$^{flox/flox}$ Embryonic Kidneys		
Mouse ID # of Pregnant Dam	**# Embryonic Kidney Pairs Pooled into FACS Sample**	**# *Cited1(+)* Cells Collected During FACS**
180-3	7	223,000
193-5	5	62,000
199-1	4	34,000
199-2	3	15,000
198-4	3	47,000
197-1	3	19,000
Total # Cells used in RNA Extraction		**400,000**

Table 1d.

Total Kidney Cell Pools Collected from *Cited1*$^{+/+}$;*R26*$^{tdTomato/+}$;*Wt1*$^{flox/flox}$ Embryos	
Mouse ID # of Pregnant Dam	**# Embryonic Kidney Pairs Pooled into Total Kidney Cell Pool Sample***
192-1	3
222-1	6
193-5	5
199-1	4
197-1	2
***1/4 of each total kidney cell pool pellet used in RNA extraction**	

Table 1e.

Hoxb7(+) Cells Collected During FACS from *Hoxb7*^{GFP} Embryonic Kidneys		
Mouse ID # of Pregnant Dam	**# Embryonic Kidney Pairs Pooled into FACS Sample**	**# *Hoxb7(+)* Cells Collected During FACS**
210-3	3	242,000
210-7	3	72,000
210-9	2	95,000
210-2	4	358,000
Total # Cells used in RNA Extraction		**767,000**

Table 1f.

Total Kidney Cell Pools Collected from *Hoxb7*$^{+/+}$ Embryos	
Mouse ID # of Pregnant Dam	**# Embryonic Kidney Pairs Pooled into Total Kidney Cell Pool Sample***
210-7	8
210-3	4
210-9	4
***1/4 of each total kidney cell pool pellet used in RNA extraction**	

2.14 Reverse Transcription of RNA from Fluorescence-Sorted Cells and Total Kidney Cell Pools of Littermates

cDNA was prepared from each RNA sample using an iScript cDNA Synthesis Kit (Bio-Rad, cat. # 1708890). For *Cited1(+)* samples and all total kidney cell pool samples from $Wt1^{+/+}$ and $Wt1^{flox/flox}$ mice, each reaction consisted of 1000 ng of RNA, 1 μL of iScript Reverse Transcriptase, 4 μL of 5x iScript Reaction Mix and nuclease-free water up to a total reaction volume of 20 μL. 500 ng of RNA was loaded into each cDNA synthesis reaction for the *Hoxb7(+)* sample and samples from total kidney cell pools of littermates. The thermal cycling conditions used in every reverse transcription reaction were: 25°C for 5 minutes, 46°C for 20 minutes, 95°C for 1 minute and holding the samples finally for an indefinite period at 4°C. All cDNA samples were diluted in water to a final concentration of 5 ng/μL.

2.15 RT-qPCR Analysis of Wildtype *Wt1* Expression in *Cited1(+)* Cells and Total Kidney Cell Pools

To ensure amplification of only the wildtype *Wt1* transcript, we used *Wt1* primers previously described in [131], which are specific to the region of *Wt1* that is excised by Cre (exons 8 and 9) in our floxed mice. The sequence of these primers and their annealing temperatures, along with all DNA repair gene primers used in subsequent RT-qPCR analyses, is given in Table 2. 10 ng of cDNA was loaded into each qPCR reaction, along with 5 μL of SsoFast EvaGreen Supermix (Bio-Rad, cat. # 1725211), Forward and Reverse primers each at a final concentration of 0.3 μM, and 2.4 μL of nuclease-free water. The total volume of each reaction was 10 μL and each reaction took place in a single well of a 96-well -qPCR plate. Quantitative measurement of *Wt1* mRNA was performed in technical triplicate for each cDNA sample, and the qPCR plate was read by a LightCycler 480 Instrument II (Roche, product # 05015278001).

2.16 RT-qPCR Analysis of DNA Repair Gene Expression in *Cited1(+)* Cells, *Hoxb7(+)* Cells and Total Kidney Cell Pools

Based on the results of the DNA repair-focused RT^2 Profiler PCR Array, which are described in section 3.1, 7 DNA repair genes were selected for further gene expression analysis in isolated cellular lineages of the embryonic kidney: *Brca1, Exo1, Lig1, Neil3, Rad18, Rad51b,* and *Ung*. The RT-qPCR primer sequences used for each of these genes are displayed in Table

2. The primers for *Brca1* and *Rad51b* were previously published [132, 133]. All other DNA repair RT-qPCR primers were either obtained from PrimerBank or designed using NCBI Primer-BLAST. The reaction volumes and reaction conditions were the same as are described in section 2.15.

Table 2. Sequences and annealing temperatures of primers used for RT-qPCR.

Gene	Forward Primer Sequence (5' -> 3')	Reverse Primer Sequence (5' -> 3')	Annealing Temperature	Source
Brca1	CGCCTCACTTTAACTGACGCAA	AGACCGGACCACCCATGAATAG	59	Serrano et al. [135]
Exo1	TGGCTGTGGATACCTACTGTT	ATCGGCTTGACCCCATAAGAC	59	PrimerBank ID: 31560511a1
Lig1	TTCTGAGCTGTGAAGGGGAG	GACGCTTTGGGAATCCTGATG	59	PrimerBank ID: 6754544a1
Neil3	TCCCTGGCTGATGTCGCTA	AGCTCCTTCCCTAAGGTTTCC	59	PrimerBank ID: 22122759a1
Rad18	GGAAGCGGCTCACAAAAATGA	TGTACGGAAAGCTGGCACAA	59	NCBI Primer-BLAST (Mouse reference sequence NM_001167730.1)
Rad51b	TGACGAATCAAATTACGACCCAT	CCTAGTGCAGCTACCAAACAG	59	Liu et al. [136]
Ung	ACCTAATCAAGCTCACGGGC	TGAGGAGGAGGACACCTTGT	59	NCBI Primer-BLAST (Mouse reference sequence NM_011677.2)
Wt1	CAAGGACTGCGAGAGAAGGTTT	TGGTGTGGGTCTTCAGATGGT	59	Hu et al.[137]
B2m	TGCAGAGTTAAGCATGCCAGTATGG	TGATGCTTGATCACATGTCTCG	59	Paul Goodyer Lab

2.17 Cryosection and Confocal Imaging of *Cited1*$^{CreER(T2)/+}$;*R26*$^{tdTomato/+}$ Embryonic Kidneys

In order to activate the fluorescence in the embryonic kidneys, a pregnant dam received an intraperitoneal injection of Tamoxifen (Sigma, product # T5648) dissolved in corn oil (10 mg per 40 g body weight) when embryos had matured to E17.5 stage of development. 24 hours post-injection, the pregnant dam was sacrificed and embryos were microdissected. Tails from each embryo were collected for genotyping by PCR. Embryonic kidneys were removed and each kidney was placed in a separate tube and rinsed in PBS (Corning). Kidneys were fixed for 3 hours in 4% PFA. Kidneys were placed in solutions of increasing sucrose concentration and eventually snap-frozen over dry ice, in cryomolds containing embedding medium for frozen tissue specimens (Sakura, item # 4583). Cryosections were prepared (Leica CM3050 S) at 7 μm thickness and VECTASHIELD mounting solution with DAPI (Vector Laboratories, cat. # H-1200), was used to coverslip the samples and stain the nuclei of the cells in the mounted cryosections. Confocal images of the cryosections were taken with a laser scanning confocal microscope (Zeiss LSM 780).

Embryo tail biopsies were genotyped by the PCR method described earlier, to confirm which embryos carried the *Cited1*$^{CreER(T2)}$ transgene insertion and would therefore be expected to have fluorescence in the CM of the kidney. The kidneys from embryos wildtype at the *Cited1* locus were used as negative controls for fluorescent imagery.

CHAPTER 3: RESULTS

3.1 DNA Repair Gene Expression in Embryonic Versus Adult Mouse Kidney (RT^2 Profiler PCR Array)

Web-based PCR array data analysis software (Qiagen web portal at GeneGlobe, http://www.qiagen.com/geneglobe) was used to interpret the controls and to quantify the fold change in expression of each DNA repair gene in embryonic kidneys compared to adult kidneys, using the delta-delta C_T method. The C_T value of each repair gene was normalized to that of *B2m*, as this was the housekeeping gene with the most consistent C_T value across all cDNA samples. All samples passed the quality controls verifying PCR array reproducibility, reverse transcription efficiency, and no genomic DNA contamination.

Supplementary Table S1 shows the fold change value for each DNA repair gene included in the RT^2 Profiler PCR Array (listed alphabetically). This fold change value represents the normalized expression for the gene of interest in the embryonic kidney divided by its normalized expression in the adult kidney. Each P-value was calculated using a Student's t-test of the normalized expression for each gene in the embryonic versus the adult kidney samples. Overall, there was a clear trend of many genes being upregulated in the embryonic kidney, compared to the adult: 48 of the 84 genes assessed in this array had a fold change value greater than 2.0, with a corresponding P-value less than 0.05. This trend is illustrated in Figure 5, which shows a scatterplot of the log-transformed normalized expression data for genes in the embryonic versus the adult kidney. Each blue dot represents a gene that is expressed greater than 2-fold higher in the embryo. Fold regulation represents the negative inverse of each fold change value lower than 1.0, and is described as a more intuitive way of presenting decreases in expression. Genes with a fold regulation value between -2 and 2 (corresponding to a fold *change* value between 0.5 and 2), are shown in red. These genes were relatively unchanged in expression level between embryo and adult. The single gene (*Parp3*) with a fold regulation value less than -2 (fold change between 0 and 0.5) is shown in green. Despite downregulation of *Parp3* in the embryo being greater than 2-fold, the corresponding P-value was greater than 0.05, therefore none of the repair genes we assessed met our criteria for downregulation in the embryo compared to the adult.

We selected genes upregulated greater than 20-fold in the embryonic kidney compared to the adult, with a corresponding P-value less than 0.05, for further study of DNA repair gene expression in specific embryonic kidney compartments. We chose this cut-off as we thought it represented a robust increase in gene expression in the embryonic kidney relative to the adult and these selection criteria left us with a good number of candidates for further expression analysis. Table 3 shows only those genes with a fold change value greater than 20 and a P-value less than 0.05. These seven genes are listed alphabetically: *Brca1, Exo1, Lig1, Neil3, Rad18, Rad51b,* and *Ung.*

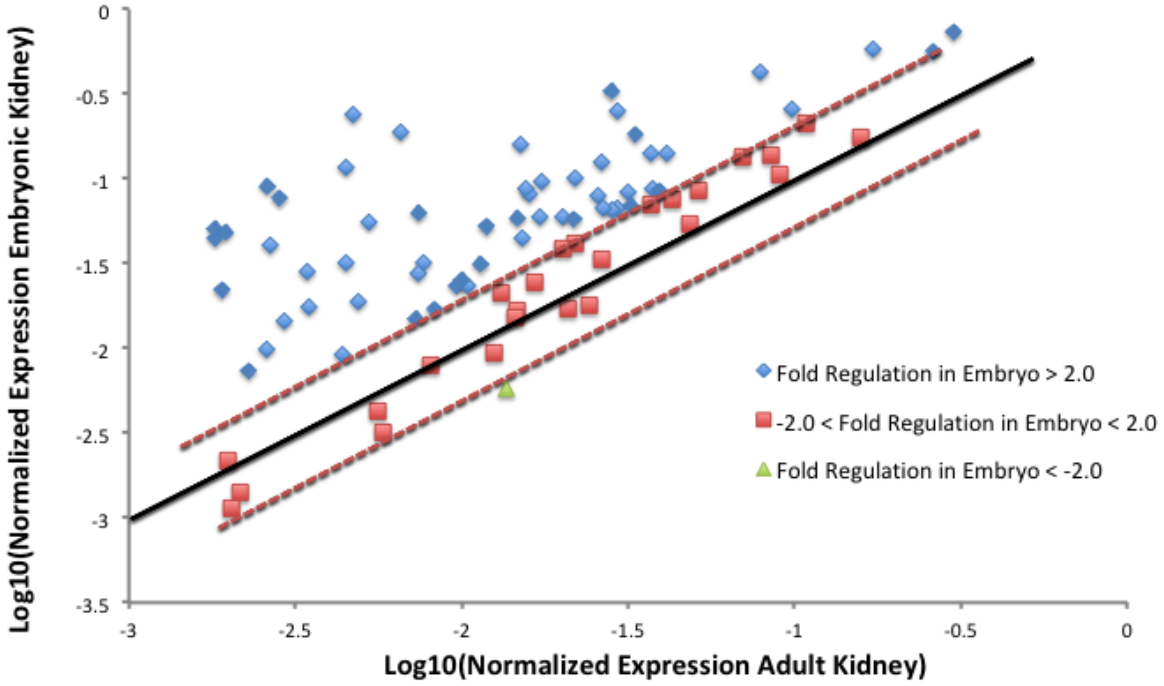

Figure 5. Normalized expression of repair genes in embryonic versus adult mouse kidney.

This scatterplot shows the log-transformed normalized expression of every DNA repair gene on the RT^2 Profiler Array. Expression in the embryonic kidney is plotted on the y-axis and expression in the adult kidney is plotted on the x-axis. Genes upregulated greater than 2-fold in the embryo are shown in blue. Genes with a fold-regulation between -2 and 2 in the embryo, representing genes relatively unchanged in expression level between embryo and adult, are shown in red. Genes with a fold-regulation value less than -2 are shown in green. These genes are under-expressed in the embryo compared to the adult.

Table 3. DNA repair genes upregulated > 20-fold in embryonic versus adult mouse kidney, with associated P-value < 0.05.

Symbol	Embryonic Kidney Fold Change (comparing to adult kidney)	P-value
Brca1	24.59	0.000162
Exo1	34.7755	0.019745
Lig1	28.5747	0.001224
Neil3	28.0514	0.003121
Rad18	25.8722	0.000154
Rad51b	24.8757	0.002358
Ung	27.1585	0.001891

This fold change value represents the normalized expression for the gene of interest in the embryonic kidney divided by its normalized expression in the adult kidney. Each P-value was calculated using a Student's t-test of the normalized expression for each gene in the embryonic versus the adult kidney samples.

3.2 Expression of DNA Repair Genes in *Cited1(+)* Cells of Embryonic Kidney Versus Total Kidney Cell Pools

The C_T value of each repair gene was normalized to that of *B2m* for every sample. The normalized expression of each repair gene in *Cited1(+)* cells was computed as a fold change relative to average expression of the gene in 6 total kidney cell pools. For 6 of the 7 DNA repair genes we looked at, we saw no enriched expression in the *Cited1* portion of the kidney: 3 of the 7 genes were expressed at similar levels in the *Cited1*-compartment and total kidney cell pools, while *Exo1*, *Rad51b* and *Ung* were all expressed at much lower levels in the *Cited1(+)* cells than in the total kidney (all had fold change values of 0.2). Notably, *Neil3* was expressed 14.9-fold higher in the *Cited1*-compartment compared to total kidney. Figure 6 displays these results.

3.3 Gene Expression Analysis in *Cited1(+)* Cells After *Wt1* Conditional Knockout

3.3.1 Expression of Wildtype *Wt1* in *Cited1(+)* Cells of $Wt1^{flox/flox}$ Mice and $Wt1^{+/+}$ Mice

The C_T value of *Wt1* was normalized to that of *B2m* for each sample. The normalized expression of *Wt1* in *Cited1(+)* cells of $Wt1^{+/+}$ mice was computed as a fold change relative to average expression of *Wt1* in 6 total kidney cell pools ($Wt1^{+/+}$ mice). Similarly, the expression of *Wt1* in *Cited1(+)* cells of $Wt1^{flox/flox}$ mice was computed as a fold change relative to average expression of *Wt1* in 5 total kidney cell pools ($Wt1^{flox/flox}$ mice). In $Wt1^{+/+}$ mice, *Wt1* expression in *Cited1(+)* cells was 3.86-fold higher than total kidney. In $Wt1^{flox/flox}$ mice, *Wt1* expression in *Cited1(+)* cells was 1.38-fold higher than total kidney. The *Wt1* enrichment in *Cited1(+)* cells of $Wt1^{flox/flox}$ mice relative to total kidney was therefore approximately 60% reduced compared to the *Cited1*-compartment enrichment of *Wt1* in $Wt1^{+/+}$ mice. These results are displayed in Figure 7.

3.3.2 DNA Repair Gene Expression in *Cited1(+)* Cells of $Wt1^{flox/flox}$ Mice

The C_T value of each repair gene was normalized to that of *B2m* for every sample. The normalized expression of each repair gene in *Cited1(+)* cells was computed as a fold change relative to average expression of the gene in 5 total kidney cell pools. As with the $Wt1^{+/+}$

mice, 6 of the 7 DNA repair genes we looked at showed no enrichment within the *Cited1(+)* portion of the kidney; 5 of the 7 genes were expressed at similar levels in the *Cited1-* compartment compared to total kidney, while the fold change value of *Rad51b* in *Cited1(+)* cells compared to total kidney was 0.5. Notably, *Neil3* was expressed 6.2-fold higher in the *Cited1*-compartment compared to total kidney. Compared to the fold change in *Neil3* expression observed in *Cited1(+)* cells of $Wt1^{+/+}$ mice, *Neil3* enrichment within the *Cited1-* compartment of $Wt1^{flox/flox}$ mice was reduced approximately 60%. Figure 8 displays these results.

3.4 DNA Repair Gene Expression in *Hoxb7(+)* Cells Versus Total Kidney Cell Pools

Again, the C_T value of each repair gene was normalized to that of *B2m* for every sample. The normalized expression of each repair gene in *Hoxb7(+)* cells was computed as a fold change relative to average expression of the gene in 3 total kidney cell pools. *Exo1, Lig1* and *Neil3* were expressed at similar levels within total kidney cells and the *Hoxb7*-compartment. *Rad18* was expressed at reduced levels in the *Hoxb7(+)* cells relative to total kidney. *Brca1, Rad51b* and *Ung* were all expressed at higher levels within the *Hoxb7*-compartment compared to total kidney. Figure 9 displays these results.

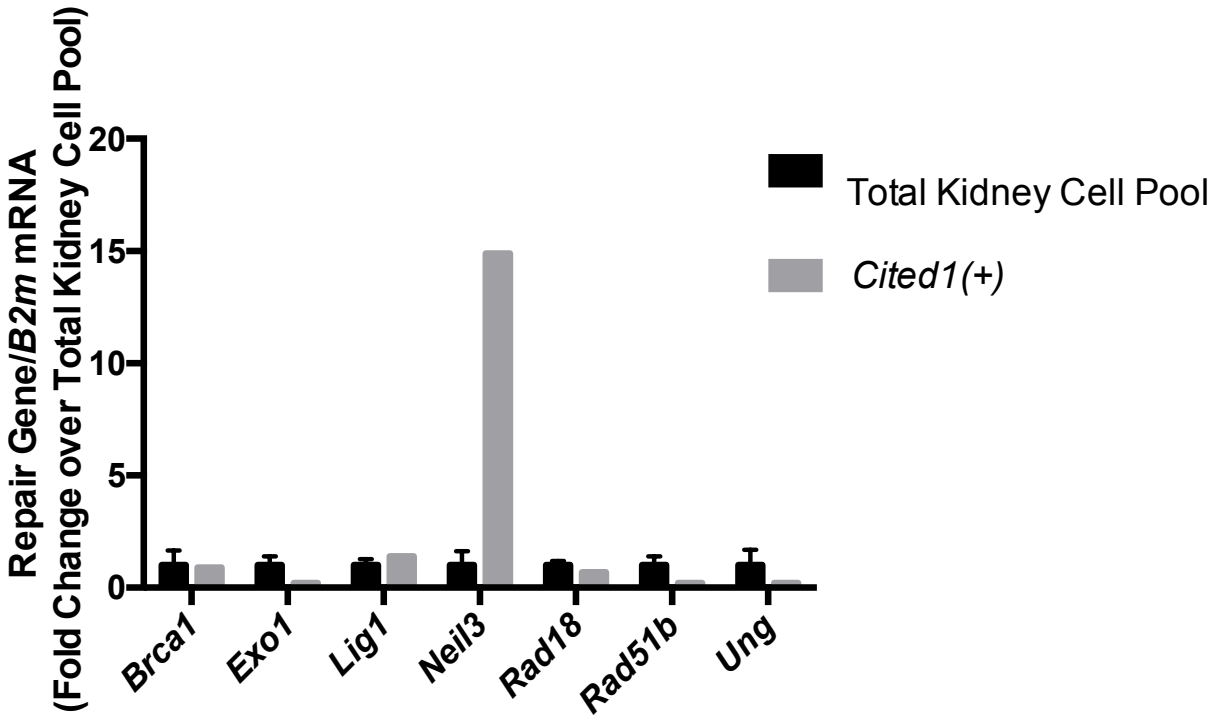

Figure 6. Fold change in DNA repair gene mRNA in *Cited1*(+) cells versus total kidney.

The expression of each repair gene was averaged across multiple pools of total kidney cells and used as a baseline against which all DNA repair gene expression measurements in the *Cited1*-compartment can be compared. The average repair gene expression in total kidney cell pools plus/minus standard error of the mean is plotted in black with the fold change in expression for the *Cited1(+)* cells shown in grey. The expression of each repair gene was normalized to *B2m* for every sample.

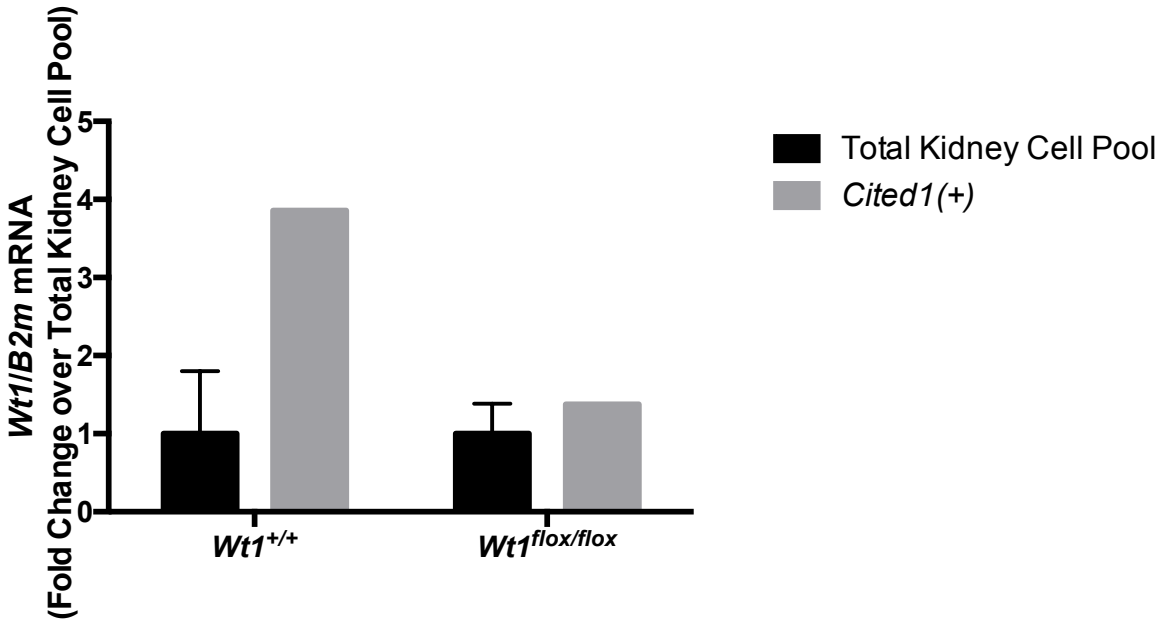

Figure 7. Fold change in *Wt1* mRNA in *Cited1(+)* cells versus total kidney for $Wt1^{+/+}$ mice and $Wt1^{flox/flox}$ mice.

The expression of wildtype *Wt1* was averaged across multiple pools of total kidney cells and used as a baseline against which all *Wt1* expression measurements in the *Cited1*-compartment can be compared. The average *Wt1* expression in total kidney cell pools plus/minus standard error of the mean is plotted in black with the fold change in expression for the *Cited1(+)* cells shown on the left for $Wt1^{+/+}$ mice and on the right for $Wt1^{flox/flox}$ mice (grey bars). The expression of *Wt1* was normalized to *B2m* for every sample.

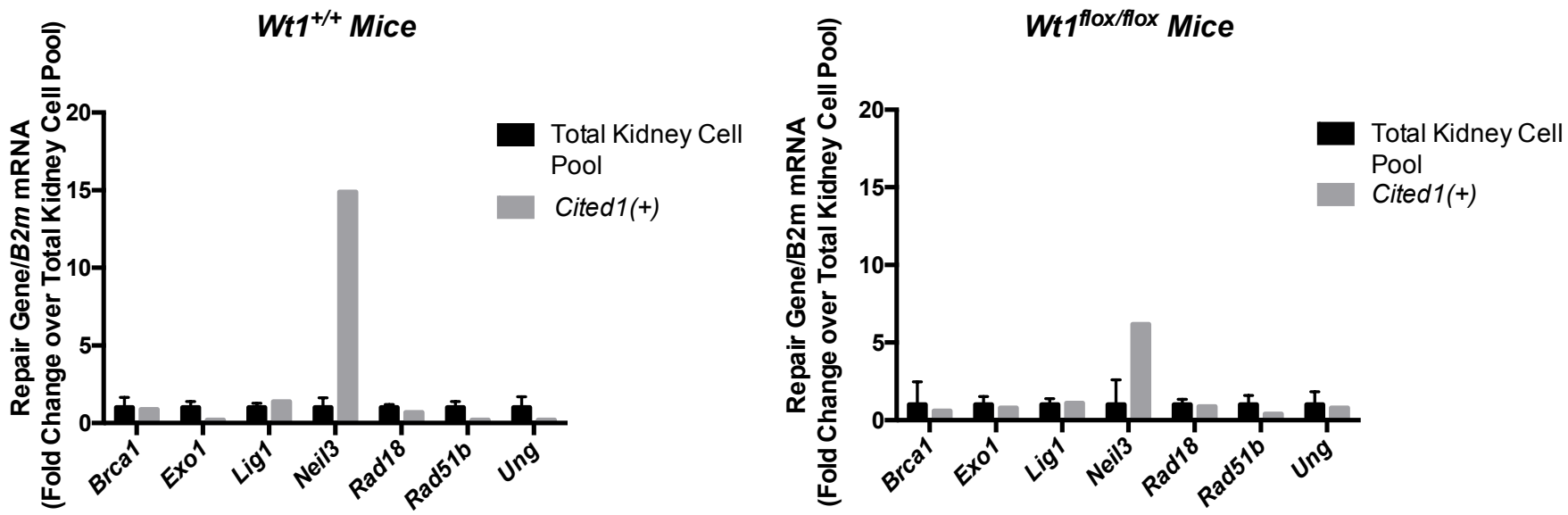

Figure 8. Fold change in DNA repair gene mRNA in *Cited1(+)* cells versus total kidney for $Wt1^{+/+}$ mice and $Wt1^{flox/flox}$ mice.

The expression of each repair gene was averaged across multiple pools of total kidney cells and used as a baseline against which all DNA repair gene expression measurements in the *Cited1*-compartment can be compared. The average repair gene expression in total kidney cell pools plus/minus standard error of the mean is plotted in black with the fold change in expression for the *Cited1(+)* cells shown on the left for $Wt1^{+/+}$ mice and on the right for $Wt1^{flox/flox}$ mice (grey bars). The expression of each repair gene was normalized to *B2m* for every sample.

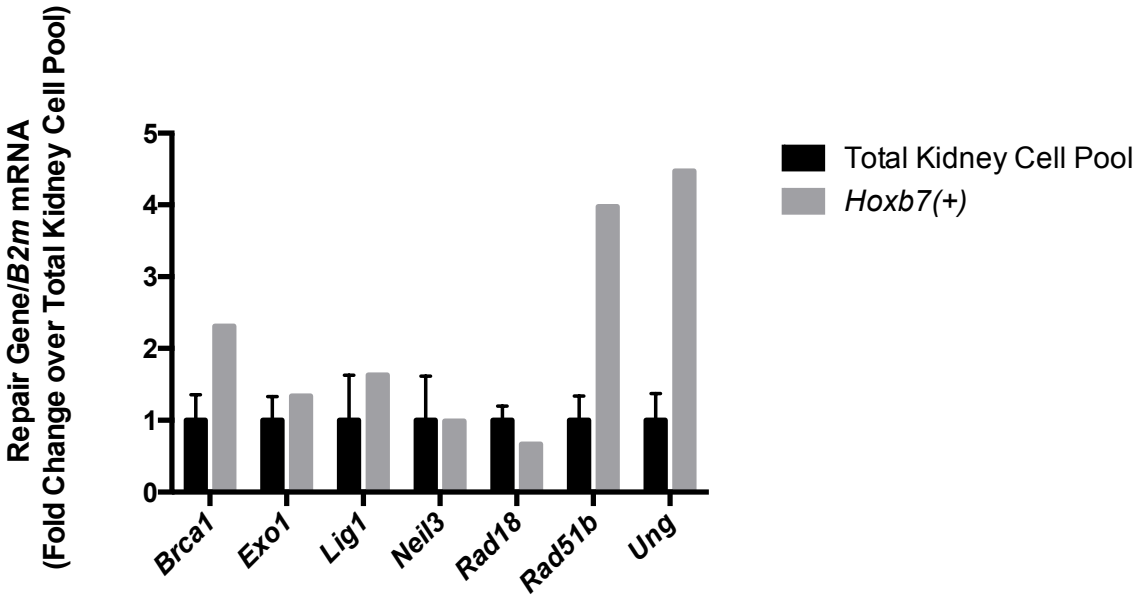

Figure 9. Fold change in DNA repair gene mRNA in *Hoxb7(+)* cells versus total kidney.

The expression of each repair gene was averaged across multiple pools of total kidney cells and used as a baseline against which all DNA repair gene expression measurements in the *Hoxb7*-compartment can be compared. The average repair gene expression in total kidney cell pools plus/minus standard error of the mean is plotted in black with the fold change in expression for the *Hoxb7(+)* cells shown in grey. The expression of each repair gene was normalized to *B2m* for every sample.

3.5 Cryosection and Confocal Imaging of *Cited1*$^{CreER(T2)/+}$;*R26*$^{tdTomato/+}$ Embryonic Kidneys

Figure 10 shows a confocal fluorescent image of a cryosection from a *Cited1*$^{CreER(T2)/+}$;*R26*$^{tdTomato/+}$ E18.5 mouse kidney. Cre recombinase was activated *in vivo* 24 hours prior to embryo dissection via intraperitoneal injection of Tamoxifen. Fluorescence is seen specifically in the CM (indicated by arrows), surrounding each branching UB tip (marked with asterisks). This image confirms that Cre recombinase is activated specifically in the CM cells, as would be expected for a gene driven under the *Cited1* promoter. 24 hours post-Tamoxifen injection, fluorescence is visible in the CM cells and, to a small extent, in the CM cells that have started to differentiate to form pre-tubular aggregate structures.

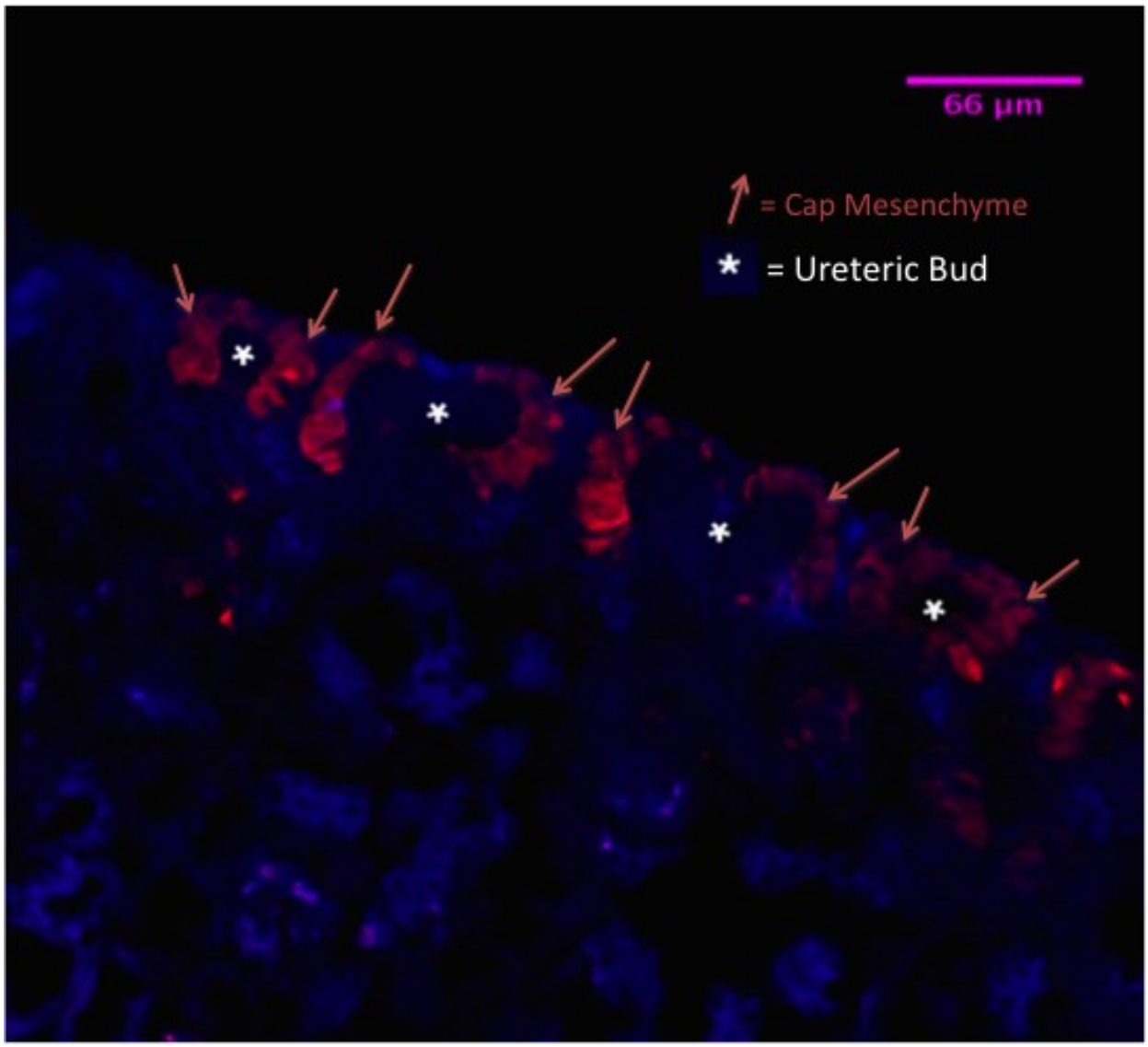

Figure 10. Confocal image of cryosection from *Cited1*$^{CreER(T2)/+;}$ *R26*$^{tdTomato/+}$ E18.5 kidney.

Pregnant dam was treated with intraperitoneal injection of Tamoxifen (10 mg per 40 g body weight) 24 hours prior to embryonic kidney harvest and preparation of cryosections. This image illustrates that expression of the red fluorescent protein, tdTomato, is specific to the cap mesenchyme structures (indicated by orange arrows) framing each ureteric bud tip (asterisks). DAPI is staining the nuclei of each cell in blue. Confocal images of the cryosections were taken with a laser scanning confocal microscope (Zeiss LSM 780).

CHAPTER 4: DISCUSSION

4.1 DNA Repair Genes Upregulated in the Embryonic Versus Adult Mouse Kidney

Using RT-qPCR analysis, we observed that many DNA repair genes (48 of 84 assessed) were expressed 2-fold greater in the embryonic kidney compared to the adult. Few studies have looked at expression of DNA repair genes within the embryonic kidney specifically; however, there are several publications investigating DNA repair gene expression in human embryonic stem cells compared to their differentiated counterparts. These studies suggest that the pluripotency and rapid division of stem cells in the human embryo make it necessary for DNA repair mechanisms to be robust in these cells [68, 134, 135]. Embryonic cells that are not yet terminally differentiated often have shorter cell cycles than differentiated cells; they are thus exposed to an increased risk of mutations during DNA replication. Furthermore, unrepaired DNA damage in these embryonic cells can result in erroneous DNA throughout an entire cell lineage. Accordingly, these studies showed that the expression of DNA repair genes (and the proteins they encode) was much higher in the undifferentiated embryonic cells compared to their differentiated equivalents [68, 134, 135]. Our RT-qPCR array compared repair gene expression in the adult kidney to that of embryonic kidney cells, which include a population of multipotent and rapidly-dividing progenitors. The previously published trend of decreased DNA repair gene expression as embryonic cells differentiate might predict that the adult kidney, comprised almost completely of terminally-differentiated cells, would have lower expression of DNA repair genes than the embryo. The results of our RT^2 Profiler array support this idea.

4.2 Enrichment of *Neil3* Expression in the *Cited1*-compartment of the Embryonic Kidney

Of the 7 DNA repair genes whose expression we examined in specific kidney compartments, only *Neil3* showed considerable enrichment in the *Cited1(+)* cells relative to total kidney cell pools. We also used the GenitoUrinary Development Molecular Anatomy Project (GUDMAP) database, http://www.gudmap.org, in May 2018, to look at previously published expression data by embryonic kidney compartment (Melissa Little group) for our selected 7 DNA repair genes [136, 137]. The *Neil3* microarray expression data published on the GUDMAP database is contradictory and difficult to interpret. 1 of 2 microarray heatmaps

shows *Neil3* expression throughout the embryonic kidney, including in the ureteric bud and interstitium; the other heatmap only shows consistent *Neil3* expression in the ureteric tip at E15.5. Ideally, we would like to have resolved the contradictory *Neil3* embryonic kidney expression data and claim definitively that *Neil3* expression is hugely enriched in the *Cited1*- compartment specifically. However, further work must first be done to validate the results we observed. One major limitation of this project was the large amount of time required to collect a sufficient number of *Cited1(+)* cells via FACS to perform RNA extraction and gene expression analysis. Consequently, it was not feasible during the preparation of this thesis, to collect multiple pools of *Cited1(+)* cells and perform the gene expression analyses multiple times. This should be the first step in confirming *Neil3* enrichment in the *Cited1*- compartment.

4.2.1 NEIL3 Structure and Function

Along with NEIL1/2, NEIL3 was first identified as a mammalian homologue to the bacterial DNA repair enzyme, endonuclease VIII (Nei) [138]. Key structural motifs were conserved between mammalian NEIL1/2/3 and the bacterial Nei protein family, and subsequent studies have shown that all three mammalian proteins have DNA glycosylase activity [139-141]. Specifically, NEIL1/2/3 act in the initial step of the BER pathway: their job is to recognize bases that have been damaged, most often by oxidation specifically, and remove the damaged base by cleaving the N-glycosidic bond between the base and the sugar in the DNA backbone [142]. Lesion repair follows the removal of the oxidized base, as described briefly in section 1.6.1.1 of this thesis.

In addition to the N-terminal domain conserved between all NEIL proteins and bacterial Nei, NEIL3 also contains an elongated C-terminal domain with unknown function [143]. Furthermore, when researchers attempted to demonstrate glycosylase activity of the three NEIL proteins, NEIL3 proved the most elusive. The first evidence that purified NEIL3 has glycosylase activity came from Takao et al., who showed that expression of recombinant NEIL3 in an nei-deficient *E. coli* strain could partially rescue the hydrogen peroxide-sensitivity phenotype [143]. Takao et al. also showed that NEIL3 had AP lyase activity when acting on single-stranded DNA, allowing removal of the abasic site from the DNA strand

[144]. Since these early studies, NEIL3 glycosylase activity has been shown to be important for removing oxidative damage, specifically within progenitor cells of the developing brain [145]: *Neil3-/-* mice are viable but neural progenitor cells lose proliferative capacity and thus cannot repair brain damage after hypoxia-ischemic events. *Neil3-/-* cells grown in culture are deficient in repair of oxidized bases within single-stranded DNA [145].

4.2.2 NEIL3 Expression Pattern

In Liu et al.'s comprehensive review of NEIL3 literature [146], the authors remark on the striking tissue specificity of NEIL3 expression, which is unexpected given the normally broad expression pattern of DNA glycosylases. Preliminary studies on expression of *Neil3* in adult mice showed that *Neil3* expression was largely restricted to testes, areas of the brain harbouring progenitor cells, and hematopoietic tissues, including spleen, thymus, blood cells, and bone marrow [143, 147, 148]. Immunofluorescent microscopy studies demonstrated NEIL3 localizes exclusively to the nucleus, consistent with a role for NEIL3 in DNA repair [147]. RT-qPCR and Northern blot studies showed that *Neil3* expression in the mouse embryo was dependent on developmental-stage and coincides with the onset of organ formation; expression increased to peak levels at E12.5 in the embryonic brain, and E15 in the mouse embryo overall [143, 149]. Interestingly, *Neil3* expression also shows dependency on the cell cycle: rapidly-dividing cells generally express *Neil3* at a higher level than cells that spend more time quiescent [147].

In the context of embryonic kidney development, we expect the nephron progenitor cells to undergo a burst of rapid division in order to generate the many millions of differentiated epithelial cells required by the nephrons of the mature kidney. While *Neil3* expression within the embryonic kidney has not been specifically studied before, the elevated expression we observed here within the nephron progenitors is consistent with prior evidence of *Neil3* expression being highest in rapidly-dividing progenitor cells [147, 149]. Liu et al. proposed that NEIL3 reinforces the oxidative damage repair system, specifically within progenitor cells of developing organs, which are exposed to the stress of frequent cell division. If that is true, it might be that compromise of this repair system, following loss of *WT1* at a critical

time in nephrogenesis, could predispose NPCs to the oncogenic mutations that drive Wilms tumor.

4.2.3 *Neil3* Expression within the *Cited1*-Compartment shows *Wt1* Dependence

We observed a 60% decrease in *Neil3* enrichment in *Cited1(+)* cells following *Wt1* conditional knockout, compared to *Cited1(+)* cells of $Wt1^{+/+}$ mice. For this reason, we believe that *Neil3* expression might be regulated by WT1. A preliminary search for WT1 transcription factor binding sites within the *Neil3* promoter region did not return any results (we checked multiple databases of transcription factor binding sites [150-152]). However, ChIP-seq studies from other researchers have demonstrated that, in its capacity as a transcription factor, WT1 often binds to distal regulatory elements, and may not bind the promoter region of a target gene directly [53]. Furthermore, it is evident that DNA-binding within regulatory regions is only one of many possible routes for WT1 to affect *Neil3* expression. In addition to its DNA-binding ability, certain splice isoforms of WT1 have also been shown to bind mRNA [54] and microRNA [57]. WT1 also participates in epigenetic modification, and, by doing so, affects the transcriptional availability of targets, such as *Wnt4* [41]. There are, therefore, multiple levels at which WT1's regulation of *Neil3* could occur. Our lab has already started to take a preliminary look at possible WT1-dependant microRNAs with seed sequences that target DNA repair genes. It will be of great interest to further explore the various mechanisms behind the observed WT1-dependence of *Neil3*.

4.2.4 NEIL3 Substrate Specificity and *CTNNB1* Mutations in Wilms Tumors

In the original study that characterized the association between mutations in exon 3 of *CTNNB1* and *WT1*-mutant Wilms tumors, 10 of the 17 tumors described carried C→T missense mutations at a codon encoding a critical phosphorylation residue of beta-catenin[2]. Interestingly, C→T transition mutations are predominant following oxidative base damage in *Escherichia coli* [153]. Liu et al. showed that NEIL3 preferentially repairs oxidative lesions, specifically the further oxidation products of 8-oxoG (a common lesion resulting from free radical attack) [141]. Therefore, it appears that the form of DNA damage preferentially repaired by NEIL3 (oxidative lesions), most frequently results in the most common type of base alteration (C→T transition) observed in the *CTNNB1* gene within *WT1*-mutant Wilms tumors.

Thus far, this remains a simple correlation and much more work will be required to determine whether C→T transitions occur at a higher frequency throughout the genome of *WT1*-mutant NPCs than in NPCs with functional WT1. If they do, it would be interesting to test whether accumulation of transition mutations in these cells could be prevented by exogenous expression of WT1, or indeed, NEIL3.

4.3 Incomplete Ablation of *Wt1* from the *Cited1*-Compartment

RT-qPCR using primers that selectively amplify wildtype *Wt1* (and not the recombined *Wt1* transcript), showed that we did not manage to completely knockout *Wt1* from *Cited1(+)* cells isolated by FACS. The 3.86-fold enrichment of *Wt1* in *Cited1(+)* cells versus total kidney of $Wt1^{+/+}$ mice was decreased to 1.38-fold enrichment in $Wt1^{flox/flox}$ mice, representing a 60% decrease in the floxed mice. We could think of a couple possible explanations for this. Firstly, within any *Cited1(+)* cell of a $Wt1^{flox/flox}$ mouse, it is possible that Cre-mediated recombination could occur at one $Wt1^{flox}$ locus but not the other. Recombination would need to occur at both loci in order to completely ablate production of *Wt1* wildtype transcript within a single cell. Prior studies using this $Cited1^{CreER(T2)};Wt1^{flox}$ system used mice with one $Wt1^{flox}$ allele and one null allele (generated by targeted mutation) [66, 129, 131]. In these studies, complete ablation of *Wt1* is more likely, as it would only require a single recombination event in each cell. Secondly, there has been no published data on the efficiency of Cre recombination at the *Wt1* locus compared to the *R26* reporter locus. Indeed, recombination at the reporter locus is used to estimate recombination efficiency at other loci of interest, under a specific Cre system. However, it is known from literature that recombination efficiency can differ between floxed loci within a cell [154]. It is therefore possible that recombination may be occurring at the *R26* reporter locus and not at the $Wt1^{flox}$ loci in some cells. The result of this would be activation of tdTomato expression and red fluorescence in a subset of *Cited1(+)* cells, but without ablation of *Wt1*. It might be necessary to repeat this study using mice with one $Wt1^{flox}$ allele and one null allele, in combination with the $Cited1^{CreER(T2)/+};R26^{tdTomato/+}$ Cre reporter system. If the incomplete *Wt1* ablation we

observed in this work was due to recombination at only one of two *Wt1*^{flox} loci, we should be able to achieve complete ablation by incorporating the *Wt1*$^{-}$ (null) allele into our model.

4.4 Cellular Pliancy and Wilms Tumorigenesis

In a review article about the genomes of solid pediatric tumors (a category which includes Wilms tumors), Chen et al. introduce the concept of cellular pliancy [155]. Cellular pliancy is explained as the characteristics of each cell type that determine whether that cell can withstand a given genetic lesion and undergo oncogenic transformation as a result. The authors argue that a specific developmental stage and cellular origin can influence the competence of the cell for transformation following loss of a tumor suppressor gene or acquisition of activating mutations. With this concept in mind, we believe that loss of *WT1* from the nephron progenitors, a cell type that exists within a narrow developmental window, creates a particular microenvironment within these cells that is suitable for malignant transformation following further genetic insult. We hypothesize that a component of this microenvironment created by *WT1*-loss is deficient DNA repair; therefore, *WT1*-mutant NPCs are not only competent for malignant transformation following further mutation, but are more likely to experience the genetic mutation events in question. Chen et al. discuss how alteration of the epigenetic landscape is an important mechanism by which specific cell types and not others become vulnerable to transformation [155]. WT1 has been shown to exert influence on the epigenetic landscape [41], therefore, it is possible that the cellular pliancy of *WT1*-mutant NPCs could be dependent on epigenetic modification following loss of *WT1*.

Cellular pliancy might also be relevant in explaining why the dysregulation of DNA repair, which we are proposing occurs in *WT1*-mutant NPCs, does not cause a broader phenotype of genomic instability beyond nephrogenesis (broad genomic instability is well-documented in other instances of deficient DNA repair [116, 117]). The cellular origin and developmental context are clearly important for Wilms tumorigenesis, as the majority of Wilms tumors are believed to initiate from a subset of renal mesenchyme cells during a specific time period within nephron development. It could be that downregulation of *NEIL3* is insufficient to cause genomic instability and subsequent oncogenesis in most contexts, however in the context of *WT1*-mutant NPCs, the microenvironment is conducive to transformation. Indeed, prior studies of *Neil3-/-*

mice suggest that loss of *Neil3* may only result in mutation accumulation in specific cell types, and does not cause genomic instability throughout the organism (in these studies, mutation accumulation within the embryonic kidney was not explicitly examined) [145].

CHAPTER 5: CONCLUSIONS AND FUTURE DIRECTIONS

5.1 Conclusions

Wilms tumor has long been used to study the parallels between embryonic kidney development and tumor formation. Similarly, in this project, we have used Wilms tumor as a frame through which we examined DNA repair during both normal kidney development and tumorigenesis.

Using a DNA-repair-focused RT-qPCR array, we defined a group of repair genes expressed at a high level in the embryonic compared to the adult mouse kidney. We described a general trend of elevated expression of genes across multiple repair pathways in the embryo versus the adult and selected 7 repair genes that were most upregulated in the embryo for further study within this project.

Using RT-qPCR, we determined that a glycosylase in the BER pathway, *Neil3,* was enriched 15-fold in the *Cited1*-compartment of the mouse embryonic kidney compared to pools of cells from the total kidney. When we examined a second embryonic kidney lineage, *Hoxb7*-expressing ureteric bud cells and their derivatives, we saw no enrichment of *Neil3* relative to total kidney cells. Indeed, while 3 of the 7 repair genes assessed showed some enrichment within the *Hoxb7*-compartment, this enrichment was nowhere close to the striking 15-fold change in expression of *Neil3* in the *Cited1(+)* cells.

In humans, oncogenic mutation of *WT1-/-* NPCs contained within the *CITED1*-compartment can give rise to Wilms tumor. Having identified *Neil3* as highly-expressed within *Cited1(+)* cells of mice, we next wanted to establish whether *Neil3* showed dependence on *Wt1* expression. We used a Cre/Lox recombination system in mice to conditionally ablate *Wt1* within the *Cited1*-compartment, followed by FACS to isolate only cells having undergone Cre-mediated recombination at a reporter locus. RT-qPCR on *Cited1(+)* cells after conditional knockout of *Wt1* showed that enrichment of *Wt1* in the *Cited1*-compartment relative to total kidney was reduced by approximately 60% compared to *Cited1(+)* cells of $Wt1^{+/+}$ mice. While we were unable to completely ablate *Wt1* from the *Cited1(+)* cells, we did see a corresponding 60% decrease in *Neil3* enrichment in the *Cited1(+)* cells with the *Wt1* conditional knockout, compared to *Cited1(+)* cells of $Wt1^{+/+}$ mice. This suggests that *Neil3* expression within the

Cited1-compartment may be dependent on *Wt1*, and is therefore an interesting candidate for investigation into a mechanism of Wilms tumorigenesis involving DNA repair deficiency.

5.2 Future Directions

5.2.1 Quantifying Expression of a Broad Panel of DNA Repair Genes in the *Cited1*-Compartment

In this project, we chose to examine kidney-compartment-specific expression of only the DNA repair genes upregulated greater than 20-fold in the embryonic compared to the adult mouse kidney. This was an arbitrary threshold that left us with a reasonable number of DNA repair genes to further investigate. However, it would be of interest to repeat the entire DNA repair-focused RT-qPCR array within the *Cited1(+)* cells to get a global view of every DNA repair gene upregulated in the *Cited1*-compartment compared to total kidney. By doing this, we might identify more WT1-dependent repair genes enriched in NPCs, which may be important in preventing Wilms tumor. If NEIL3 does indeed act as a second line of defense against oxidative DNA damage in NPCs [146], what is the primary line of defense against oxidative damage in these cells? We might expect the expression of other BER genes enriched in the *Cited1*-compartment to be dependent on WT1.

5.2.2 Confirming NEIL3 Protein Localization within the Embryonic Kidney

Thus far, we have only provided evidence of enriched *Neil3* expression in the *Cited1*-compartment at the mRNA level. It is common knowledge that mRNA expression does not always equate with protein levels, and it will therefore be important to determine whether NEIL3 protein is enriched in the *Cited1(+)* cells of the embryonic kidney relative to the whole kidney. To assess this, we will use immunofluorescence microscopy on E18.5 embryonic kidney cryosections from our *Cited1*$^{CreER(T2)/+}$;*R26*$^{tdTomato/+}$mice (preparation of these cryosections is described in section 2.17 of this thesis). We will use a fluorescently-tagged antibody raised against mouse NEIL3 and look for colocalization of the NEIL3 signal with the fluorescent tdTomato signal in the CM.

5.2.3 Assessing DNA Repair Gene Expression in *WT1*-Mutant Tumors

We could extend our findings to predict that *WT1*-mutant Wilms tumors have reduced *NEIL3* expression compared to total embryonic kidney in humans. If *NEIL3* expression is WT1-dependant, as our results suggest, we would expect tumors derived from *WT1*-mutant NPCs to have low *NEIL3* expression. However, in *WT1*-wildtype total embryonic kidney, *NEIL3* should be strongly expressed following activation by WT1. We would expect only DNA repair genes that are putatively dependent on WT1 (for example, *NEIL3*), but not WT1-independent genes, to show decreased expression in *WT1*-mutant tumors versus total embryonic kidney.

REFERENCES

1. Fukuzawa, R., et al., *Sequential WT1 and CTNNB1 mutations and alterations of beta-catenin localisation in intralobar nephrogenic rests and associated Wilms tumours: two case studies.* J Clin Pathol, 2007. **60**(9): p. 1013-6.
2. Maiti, S., et al., *Frequent association of beta-catenin and WT1 mutations in Wilms tumors.* Cancer Res, 2000. **60**(22): p. 6288-92.
3. Park, S., et al., *Inactivation of WT1 in nephrogenic rests, genetic precursors to Wilms' tumour.* Nat Genet, 1993. **5**(4): p. 363-7.
4. Hoeijmakers, J.H., *Genome maintenance mechanisms for preventing cancer.* Nature, 2001. **411**(6835): p. 366-74.
5. Ahadova, A., et al., *CTNNB1-mutant colorectal carcinomas with immediate invasive growth: a model of interval cancers in Lynch syndrome.* Fam Cancer, 2016. **15**(4): p. 579-86.
6. Castiglia, D., et al., *Concomitant activation of Wnt pathway and loss of mismatch repair function in human melanoma.* Genes Chromosomes Cancer, 2008. **47**(7): p. 614-24.
7. Mugford, J.W., et al., *Osr1 expression demarcates a multi-potent population of intermediate mesoderm that undergoes progressive restriction to an Osr1-dependent nephron progenitor compartment within the mammalian kidney.* Dev Biol, 2008. **324**(1): p. 88-98.
8. Boyle, S., et al., *Cited1 and Cited2 are differentially expressed in the developing kidney but are not required for nephrogenesis.* Dev Dyn, 2007. **236**(8): p. 2321-30.
9. Self, M., et al., *Six2 is required for suppression of nephrogenesis and progenitor renewal in the developing kidney.* EMBO J, 2006. **25**(21): p. 5214-28.
10. Srinivas, S., et al., *Dominant effects of RET receptor misexpression and ligand-independent RET signaling on ureteric bud development.* Development, 1999. **126**(7): p. 1375-86.
11. Grobstein, C., *Inductive epitheliomesenchymal interaction in cultured organ rudiments of the mouse.* Science, 1953. **118**(3054): p. 52-5.
12. Erickson, R.A., *Inductive interactions in the develoment of the mouse metanephros.* J Exp Zool, 1968. **169**(1): p. 33-42.
13. Mugford, J.W., et al., *High-resolution gene expression analysis of the developing mouse kidney defines novel cellular compartments within the nephron progenitor population.* Dev Biol, 2009. **333**(2): p. 312-23.
14. Moritz, K.M., et al., *Factors influencing mammalian kidney development: implications for health in adult life.* Adv Anat Embryol Cell Biol, 2008. **196**: p. 1-78.
15. Mari, C. and P. Winyard, *Concise Review: Understanding the Renal Progenitor Cell Niche In Vivo to Recapitulate Nephrogenesis In Vitro.* Stem Cells Transl Med, 2015. **4**(12): p. 1463-71.
16. O'Brien, L.L. and A.P. McMahon, *Induction and patterning of the metanephric nephron.* Semin Cell Dev Biol, 2014. **36**: p. 31-8.
17. Kobayashi, A., et al., *Six2 defines and regulates a multipotent self-renewing nephron progenitor population throughout mammalian kidney development.* Cell Stem Cell, 2008. **3**(2): p. 169-81.

18. Boyle, S., et al., *Fate mapping using Cited1-CreERT2 mice demonstrates that the cap mesenchyme contains self-renewing progenitor cells and gives rise exclusively to nephronic epithelia.* Dev Biol, 2008. **313**(1): p. 234-45.
19. Brown, A.C., et al., *Role for compartmentalization in nephron progenitor differentiation.* Proc Natl Acad Sci U S A, 2013. **110**(12): p. 4640-5.
20. Willert, K. and K.A. Jones, *Wnt signaling: is the party in the nucleus?* Genes Dev, 2006. **20**(11): p. 1394-404.
21. Halt, K. and S. Vainio, *Coordination of kidney organogenesis by Wnt signaling.* Pediatr Nephrol, 2014. **29**(4): p. 737-44.
22. Iglesias, D.M., et al., *Canonical WNT signaling during kidney development.* Am J Physiol Renal Physiol, 2007. **293**(2): p. F494-500.
23. Carroll, T.J., et al., *Wnt9b plays a central role in the regulation of mesenchymal to epithelial transitions underlying organogenesis of the mammalian urogenital system.* Dev Cell, 2005. **9**(2): p. 283-92.
24. Cadoret, A., et al., *Hepatomegaly in transgenic mice expressing an oncogenic form of beta-catenin.* Cancer Res, 2001. **61**(8): p. 3245-9.
25. Miyoshi, Y., et al., *Activation of the beta-catenin gene in primary hepatocellular carcinomas by somatic alterations involving exon 3.* Cancer Res, 1998. **58**(12): p. 2524-7.
26. Morin, P.J., et al., *Activation of beta-catenin-Tcf signaling in colon cancer by mutations in beta-catenin or APC.* Science, 1997. **275**(5307): p. 1787-90.
27. Moon, R.T., et al., *WNT and beta-catenin signalling: diseases and therapies.* Nat Rev Genet, 2004. **5**(9): p. 691-701.
28. Giles, R.H., J.H. van Es, and H. Clevers, *Caught up in a Wnt storm: Wnt signaling in cancer.* Biochim Biophys Acta, 2003. **1653**(1): p. 1-24.
29. Kreidberg, J.A., et al., *WT-1 is required for early kidney development.* Cell, 1993. **74**(4): p. 679-91.
30. Pritchard-Jones, K., et al., *The candidate Wilms' tumour gene is involved in genitourinary development.* Nature, 1990. **346**(6280): p. 194-7.
31. Donovan, M.J., et al., *Initial differentiation of the metanephric mesenchyme is independent of WT1 and the ureteric bud.* Dev Genet, 1999. **24**(3-4): p. 252-62.
32. Davies, J.A., et al., *Development of an siRNA-based method for repressing specific genes in renal organ culture and its use to show that the Wt1 tumour suppressor is required for nephron differentiation.* Hum Mol Genet, 2004. **13**(2): p. 235-46.
33. Berry, R.L., et al., *Deducing the stage of origin of Wilms' tumours from a developmental series of Wt1-mutant mice.* Dis Model Mech, 2015. **8**(8): p. 903-17.
34. Hartwig, S., et al., *Genomic characterization of Wilms' tumor suppressor 1 targets in nephron progenitor cells during kidney development.* Development, 2010. **137**(7): p. 1189-203.
35. Akpa, M.M., et al., *Wilms tumor suppressor, WT1, suppresses epigenetic silencing of the beta-catenin gene.* J Biol Chem, 2015. **290**(4): p. 2279-88.
36. Guo, J.K., et al., *WT1 is a key regulator of podocyte function: reduced expression levels cause crescentic glomerulonephritis and mesangial sclerosis.* Hum Mol Genet, 2002. **11**(6): p. 651-9.
37. Hohenstein, P. and N.D. Hastie, *The many facets of the Wilms' tumour gene, WT1.* Hum Mol Genet, 2006. **15 Spec No 2**: p. R196-201.

38. Lefebvre, J., et al., *Alternatively spliced isoforms of WT1 control podocyte-specific gene expression.* Kidney Int, 2015. **88**(2): p. 321-31.
39. Hewitt, S.M., et al., *Differential function of Wilms' tumor gene WT1 splice isoforms in transcriptional regulation.* J Biol Chem, 1996. **271**(15): p. 8588-92.
40. Bor, Y.C., et al., *The Wilms' tumor 1 (WT1) gene (+KTS isoform) functions with a CTE to enhance translation from an unspliced RNA with a retained intron.* Genes Dev, 2006. **20**(12): p. 1597-608.
41. Essafi, A., et al., *A wt1-controlled chromatin switching mechanism underpins tissue-specific wnt4 activation and repression.* Dev Cell, 2011. **21**(3): p. 559-74.
42. Morrison, A.A., et al., *The Wilms tumour suppressor protein WT1 (+KTS isoform) binds alpha-actinin 1 mRNA via its zinc-finger domain.* Biochem Cell Biol, 2006. **84**(5): p. 789-98.
43. Szemes, M., et al., *Control of epigenetic states by WT1 via regulation of de novo DNA methyltransferase 3A.* Hum Mol Genet, 2013. **22**(1): p. 74-83.
44. Maheswaran, S., et al., *Inhibition of cellular proliferation by the Wilms tumor suppressor WT1 requires association with the inducible chaperone Hsp70.* Genes Dev, 1998. **12**(8): p. 1108-20.
45. Rong, Y., et al., *Wilms' tumor 1 and signal transducers and activators of transcription 3 synergistically promote cell proliferation: a possible mechanism in sporadic Wilms' tumor.* Cancer Res, 2006. **66**(16): p. 8049-57.
46. Discenza, M.T., et al., *WT1 is a modifier of the Pax2 mutant phenotype: cooperation and interaction between WT1 and Pax2.* Oncogene, 2003. **22**(50): p. 8145-55.
47. Discenza, M.T. and J. Pelletier, *Insights into the physiological role of WT1 from studies of genetically modified mice.* Physiol Genomics, 2004. **16**(3): p. 287-300.
48. Toska, E. and S.G. Roberts, *Mechanisms of transcriptional regulation by WT1 (Wilms' tumour 1).* Biochem J, 2014. **461**(1): p. 15-32.
49. Nakagama, H., et al., *Sequence and structural requirements for high-affinity DNA binding by the WT1 gene product.* Mol Cell Biol, 1995. **15**(3): p. 1489-98.
50. Ryan, G., et al., *Repression of Pax-2 by WT1 during normal kidney development.* Development, 1995. **121**(3): p. 867-75.
51. Kann, M., et al., *Genome-Wide Analysis of Wilms' Tumor 1-Controlled Gene Expression in Podocytes Reveals Key Regulatory Mechanisms.* J Am Soc Nephrol, 2015. **26**(9): p. 2097-104.
52. Ullmark, T., et al., *Distinct global binding patterns of the Wilms tumor gene 1 (WT1) -KTS and +KTS isoforms in leukemic cells.* Haematologica, 2017. **102**(2): p. 336-345.
53. Motamedi, F.J., et al., *WT1 controls antagonistic FGF and BMP-pSMAD pathways in early renal progenitors.* Nat Commun, 2014. **5**: p. 4444.
54. Caricasole, A., et al., *RNA binding by the Wilms tumor suppressor zinc finger proteins.* Proc Natl Acad Sci U S A, 1996. **93**(15): p. 7562-6.
55. Davies, R.C., et al., *WT1 interacts with the splicing factor U2AF65 in an isoform-dependent manner and can be incorporated into spliceosomes.* Genes Dev, 1998. **12**(20): p. 3217-25.
56. Little, N.A., N.D. Hastie, and R.C. Davies, *Identification of WTAP, a novel Wilms' tumour 1-associating protein.* Hum Mol Genet, 2000. **9**(15): p. 2231-9.

57. Akpa, M.M., et al., *Wilms Tumor Suppressor, WT1, Cooperates with MicroRNA-26a and MicroRNA-101 to Suppress Translation of the Polycomb Protein, EZH2, in Mesenchymal Stem Cells.* J Biol Chem, 2016. **291**(8): p. 3785-95.
58. Kreidberg, J.A., *WT1 and kidney progenitor cells.* Organogenesis, 2010. **6**(2): p. 61-70.
59. Call, K.M., et al., *Isolation and characterization of a zinc finger polypeptide gene at the human chromosome 11 Wilms' tumor locus.* Cell, 1990. **60**(3): p. 509-20.
60. Haber, D.A., et al., *Alternative splicing and genomic structure of the Wilms tumor gene WT1.* Proc Natl Acad Sci U S A, 1991. **88**(21): p. 9618-22.
61. Ruteshouser, E.C., S.M. Robinson, and V. Huff, *Wilms tumor genetics: mutations in WT1, WTX, and CTNNB1 account for only about one-third of tumors.* Genes Chromosomes Cancer, 2008. **47**(6): p. 461-70.
62. Little, M. and C. Wells, *A clinical overview of WT1 gene mutations.* Hum Mutat, 1997. **9**(3): p. 209-25.
63. Knudson, A.G., Jr., *Mutation and cancer: statistical study of retinoblastoma.* Proc Natl Acad Sci U S A, 1971. **68**(4): p. 820-3.
64. Knudson, A.G., Jr. and L.C. Strong, *Mutation and cancer: a model for Wilms' tumor of the kidney.* J Natl Cancer Inst, 1972. **48**(2): p. 313-24.
65. Li, C.M., et al., *CTNNB1 mutations and overexpression of Wnt/beta-catenin target genes in WT1-mutant Wilms' tumors.* Am J Pathol, 2004. **165**(6): p. 1943-53.
66. Huang, L., et al., *Nephron Progenitor But Not Stromal Progenitor Cells Give Rise to Wilms Tumors in Mouse Models with beta-Catenin Activation or Wt1 Ablation and Igf2 Upregulation.* Neoplasia, 2016. **18**(2): p. 71-81.
67. Vinson, R.K. and B.F. Hales, *DNA repair during organogenesis.* Mutat Res, 2002. **509**(1-2): p. 79-91.
68. Rocha, C.R., et al., *The role of DNA repair in the pluripotency and differentiation of human stem cells.* Mutat Res, 2013. **752**(1): p. 25-35.
69. Jaroudi, S. and S. SenGupta, *DNA repair in mammalian embryos.* Mutat Res, 2007. **635**(1): p. 53-77.
70. Luo, G., et al., *Disruption of mRad50 causes embryonic stem cell lethality, abnormal embryonic development, and sensitivity to ionizing radiation.* Proc Natl Acad Sci U S A, 1999. **96**(13): p. 7376-81.
71. Kabir, M., et al., *Properties of genes essential for mouse development.* PLoS One, 2017. **12**(5): p. e0178273.
72. Li, W. and J.C. Wang, *Mammalian DNA topoisomerase IIIalpha is essential in early embryogenesis.* Proc Natl Acad Sci U S A, 1998. **95**(3): p. 1010-3.
73. Kuznetsov, S.G., et al., *Loss of Rad51c leads to embryonic lethality and modulation of Trp53-dependent tumorigenesis in mice.* Cancer Res, 2009. **69**(3): p. 863-72.
74. Deng, C.X., *Tumor formation in Brca1 conditional mutant mice.* Environ Mol Mutagen, 2002. **39**(2-3): p. 171-7.
75. Weng, Y. and M.A. Sirover, *Developmental regulation of the base excision repair enzyme uracil DNA glycosylase in the rat.* Mutat Res, 1993. **293**(2): p. 133-41.
76. Taylor, E.M. and A.R. Lehmann, *Conservation of eukaryotic DNA repair mechanisms.* Int J Radiat Biol, 1998. **74**(3): p. 277-86.
77. Robertson, A.B., et al., *DNA repair in mammalian cells: Base excision repair: the long and short of it.* Cell Mol Life Sci, 2009. **66**(6): p. 981-93.

78. Lindahl, T., *Instability and decay of the primary structure of DNA.* Nature, 1993. **362**(6422): p. 709-15.
79. Wallace, S.S., *Base excision repair: a critical player in many games.* DNA Repair (Amst), 2014. **19**: p. 14-26.
80. Lindahl, T., *An N-glycosidase from Escherichia coli that releases free uracil from DNA containing deaminated cytosine residues.* Proc Natl Acad Sci U S A, 1974. **71**(9): p. 3649-53.
81. Klungland, A. and T. Lindahl, *Second pathway for completion of human DNA base excision-repair: reconstitution with purified proteins and requirement for DNase IV (FEN1).* EMBO J, 1997. **16**(11): p. 3341-8.
82. Tebbs, R.S., et al., *Requirement for the Xrcc1 DNA base excision repair gene during early mouse development.* Dev Biol, 1999. **208**(2): p. 513-29.
83. Xie, Y., et al., *Deficiencies in mouse Myh and Ogg1 result in tumor predisposition and G to T mutations in codon 12 of the K-ras oncogene in lung tumors.* Cancer Res, 2004. **64**(9): p. 3096-102.
84. Chan, M.K., et al., *Targeted deletion of the genes encoding NTH1 and NEIL1 DNA N-glycosylases reveals the existence of novel carcinogenic oxidative damage to DNA.* DNA Repair (Amst), 2009. **8**(7): p. 786-94.
85. Weren, R.D., et al., *A germline homozygous mutation in the base-excision repair gene NTHL1 causes adenomatous polyposis and colorectal cancer.* Nat Genet, 2015. **47**(6): p. 668-71.
86. Setlow, R.B., P.A. Swenson, and W.L. Carrier, *Thymine Dimers and Inhibition of DNA Synthesis by Ultraviolet Irradiation of Cells.* Science, 1963. **142**(3598): p. 1464-6.
87. Scharer, O.D., *Nucleotide excision repair in eukaryotes.* Cold Spring Harb Perspect Biol, 2013. **5**(10): p. a012609.
88. Boyce, R.P. and P. Howard-Flanders, *Release of Ultraviolet Light-Induced Thymine Dimers from DNA in E. Coli K-12.* Proc Natl Acad Sci U S A, 1964. **51**: p. 293-300.
89. Spivak, G., *Nucleotide excision repair in humans.* DNA Repair (Amst), 2015. **36**: p. 13-8.
90. Pettijohn, D. and P. Hanawalt, *Evidence for Repair-Replication of Ultraviolet Damaged DNA in Bacteria.* J Mol Biol, 1964. **9**: p. 395-410.
91. Reardon, J.T., et al., *In vitro repair of oxidative DNA damage by human nucleotide excision repair system: possible explanation for neurodegeneration in xeroderma pigmentosum patients.* Proc Natl Acad Sci U S A, 1997. **94**(17): p. 9463-8.
92. de Waard, H., et al., *Cell-type-specific consequences of nucleotide excision repair deficiencies: Embryonic stem cells versus fibroblasts.* DNA Repair (Amst), 2008. **7**(10): p. 1659-69.
93. Van Sloun, P.P., et al., *The role of nucleotide excision repair in protecting embryonic stem cells from genotoxic effects of UV-induced DNA damage.* Nucleic Acids Res, 1999. **27**(16): p. 3276-82.
94. Theil, A.F., et al., *Disruption of TTDA results in complete nucleotide excision repair deficiency and embryonic lethality.* PLoS Genet, 2013. **9**(4): p. e1003431.
95. Cleaver, J.E., *Defective repair replication of DNA in xeroderma pigmentosum.* Nature, 1968. **218**(5142): p. 652-6.

96. Kraemer, K.H., et al., *The role of sunlight and DNA repair in melanoma and nonmelanoma skin cancer. The xeroderma pigmentosum paradigm.* Arch Dermatol, 1994. **130**(8): p. 1018-21.
97. van Steeg, H., L.H. Mullenders, and J. Vijg, *Mutagenesis and carcinogenesis in nucleotide excision repair-deficient XPA knock out mice.* Mutat Res, 2000. **450**(1-2): p. 167-80.
98. Rich, T., R.L. Allen, and A.H. Wyllie, *Defying death after DNA damage.* Nature, 2000. **407**(6805): p. 777-83.
99. Khanna, K.K. and S.P. Jackson, *DNA double-strand breaks: signaling, repair and the cancer connection.* Nat Genet, 2001. **27**(3): p. 247-54.
100. Lindahl, T. and R.D. Wood, *Quality control by DNA repair.* Science, 1999. **286**(5446): p. 1897-905.
101. Haber, J.E., *Partners and pathwaysrepairing a double-strand break.* Trends Genet, 2000. **16**(6): p. 259-64.
102. Tichy, E.D., et al., *Mouse embryonic stem cells, but not somatic cells, predominantly use homologous recombination to repair double-strand DNA breaks.* Stem Cells Dev, 2010. **19**(11): p. 1699-711.
103. Essers, J., et al., *Homologous and non-homologous recombination differentially affect DNA damage repair in mice.* EMBO J, 2000. **19**(7): p. 1703-10.
104. Liang, F., et al., *Homology-directed repair is a major double-strand break repair pathway in mammalian cells.* Proc Natl Acad Sci U S A, 1998. **95**(9): p. 5172-7.
105. Miki, Y., et al., *A strong candidate for the breast and ovarian cancer susceptibility gene BRCA1.* Science, 1994. **266**(5182): p. 66-71.
106. Wooster, R., et al., *Localization of a breast cancer susceptibility gene, BRCA2, to chromosome 13q12-13.* Science, 1994. **265**(5181): p. 2088-90.
107. Hall, J.M., et al., *Linkage of early-onset familial breast cancer to chromosome 17q21.* Science, 1990. **250**(4988): p. 1684-9.
108. Hiramoto, T., et al., *Mutations of a novel human RAD54 homologue, RAD54B, in primary cancer.* Oncogene, 1999. **18**(22): p. 3422-6.
109. Barnes, D.E., et al., *Targeted disruption of the gene encoding DNA ligase IV leads to lethality in embryonic mice.* Curr Biol, 1998. **8**(25): p. 1395-8.
110. Jackson, S.P., *Sensing and repairing DNA double-strand breaks.* Carcinogenesis, 2002. **23**(5): p. 687-96.
111. Lees-Miller, S.P., et al., *Absence of p350 subunit of DNA-activated protein kinase from a radiosensitive human cell line.* Science, 1995. **267**(5201): p. 1183-5.
112. Riballo, E., et al., *Identification of a defect in DNA ligase IV in a radiosensitive leukaemia patient.* Curr Biol, 1999. **9**(13): p. 699-702.
113. Schaaper, R.M. and R.L. Dunn, *Spectra of spontaneous mutations in Escherichia coli strains defective in mismatch correction: the nature of in vivo DNA replication errors.* Proc Natl Acad Sci U S A, 1987. **84**(17): p. 6220-4.
114. Lu, A.L., S. Clark, and P. Modrich, *Methyl-directed repair of DNA base-pair mismatches in vitro.* Proc Natl Acad Sci U S A, 1983. **80**(15): p. 4639-43.
115. New, L., K. Liu, and G.F. Crouse, *The yeast gene MSH3 defines a new class of eukaryotic MutS homologues.* Mol Gen Genet, 1993. **239**(1-2): p. 97-108.
116. Loeb, L.A., *Mutator phenotype may be required for multistage carcinogenesis.* Cancer Res, 1991. **51**(12): p. 3075-9.

117. Buermeyer, A.B., et al., *Mammalian DNA mismatch repair.* Annu Rev Genet, 1999. **33**: p. 533-64.
118. Richman, S., *Deficient mismatch repair: Read all about it (Review).* Int J Oncol, 2015. **47**(4): p. 1189-202.
119. Peltomaki, P. and H. Vasen, *Mutations associated with HNPCC predisposition -- Update of ICG-HNPCC/INSiGHT mutation database.* Dis Markers, 2004. **20**(4-5): p. 269-76.
120. Lee, K., E. Tosti, and W. Edelmann, *Mouse models of DNA mismatch repair in cancer research.* DNA Repair (Amst), 2016. **38**: p. 140-6.
121. Meira, L.B., et al., *Mice defective in the mismatch repair gene Msh2 show increased predisposition to UVB radiation-induced skin cancer.* DNA Repair (Amst), 2002. **1**(11): p. 929-34.
122. Russo, M.T., et al., *Different DNA repair strategies to combat the threat from 8-oxoguanine.* Mutat Res, 2007. **614**(1-2): p. 69-76.
123. Reid, S., et al., *Biallelic BRCA2 mutations are associated with multiple malignancies in childhood including familial Wilms tumour.* J Med Genet, 2005. **42**(2): p. 147-51.
124. Bardeesy, N., et al., *Anaplastic Wilms' tumour, a subtype displaying poor prognosis, harbours p53 gene mutations.* Nat Genet, 1994. **7**(1): p. 91-7.
125. Smith, M.L. and Y.R. Seo, *p53 regulation of DNA excision repair pathways.* Mutagenesis, 2002. **17**(2): p. 149-56.
126. Diniz, G., et al., *Tissue expression of MLH1, PMS2, MSH2, and MSH6 proteins and prognostic value of microsatellite instability in Wilms tumor: experience of 45 cases.* Pediatr Hematol Oncol, 2013. **30**(4): p. 273-84.
127. Aaltonen, L.A., et al., *Clues to the pathogenesis of familial colorectal cancer.* Science, 1993. **260**(5109): p. 812-6.
128. Silva, F.C., et al., *Mismatch repair genes in Lynch syndrome: a review.* Sao Paulo Med J, 2009. **127**(1): p. 46-51.
129. Gao, F., et al., *The Wilms tumor gene, Wt1, is required for Sox9 expression and maintenance of tubular architecture in the developing testis.* Proc Natl Acad Sci U S A, 2006. **103**(32): p. 11987-92.
130. Srinivas, S., et al., *Expression of green fluorescent protein in the ureteric bud of transgenic mice: a new tool for the analysis of ureteric bud morphogenesis.* Dev Genet, 1999. **24**(3-4): p. 241-51.
131. Hu, Q., et al., *Wt1 ablation and Igf2 upregulation in mice result in Wilms tumors with elevated ERK1/2 phosphorylation.* J Clin Invest, 2011. **121**(1): p. 174-83.
132. Liu, Q., et al., *A miR-590/Acvr2a/Rad51b axis regulates DNA damage repair during mESC proliferation.* Stem Cell Reports, 2014. **3**(6): p. 1103-17.
133. Serrano, L., et al., *Homologous recombination conserves DNA sequence integrity throughout the cell cycle in embryonic stem cells.* Stem Cells Dev, 2011. **20**(2): p. 363-74.
134. Maynard, S., et al., *Human embryonic stem cells have enhanced repair of multiple forms of DNA damage.* Stem Cells, 2008. **26**(9): p. 2266-74.
135. Momcilovic, O., et al., *DNA damage responses in human induced pluripotent stem cells and embryonic stem cells.* PLoS One, 2010. **5**(10): p. e13410.
136. Harding, S.D., et al., *The GUDMAP database--an online resource for genitourinary research.* Development, 2011. **138**(13): p. 2845-53.

137. McMahon, A.P., et al., *GUDMAP: the genitourinary developmental molecular anatomy project.* J Am Soc Nephrol, 2008. **19**(4): p. 667-71.
138. Takao, M., et al., *A back-up glycosylase in Nth1 knock-out mice is a functional Nei (endonuclease VIII) homologue.* J Biol Chem, 2002. **277**(44): p. 42205-13.
139. Bandaru, V., et al., *A novel human DNA glycosylase that removes oxidative DNA damage and is homologous to Escherichia coli endonuclease VIII.* DNA Repair (Amst), 2002. **1**(7): p. 517-29.
140. Hazra, T.K., et al., *Identification and characterization of a novel human DNA glycosylase for repair of cytosine-derived lesions.* J Biol Chem, 2002. **277**(34): p. 30417-20.
141. Liu, M., et al., *The mouse ortholog of NEIL3 is a functional DNA glycosylase in vitro and in vivo.* Proc Natl Acad Sci U S A, 2010. **107**(11): p. 4925-30.
142. David, S.S., V.L. O'Shea, and S. Kundu, *Base-excision repair of oxidative DNA damage.* Nature, 2007. **447**(7147): p. 941-50.
143. Takao, M., et al., *Human Nei-like protein NEIL3 has AP lyase activity specific for single-stranded DNA and confers oxidative stress resistance in Escherichia coli mutant.* Genes Cells, 2009. **14**(2): p. 261-70.
144. Takao, M., et al., *Novel nuclear and mitochondrial glycosylases revealed by disruption of the mouse Nth1 gene encoding an endonuclease III homolog for repair of thymine glycols.* EMBO J, 2002. **21**(13): p. 3486-93.
145. Sejersted, Y., et al., *Endonuclease VIII-like 3 (Neil3) DNA glycosylase promotes neurogenesis induced by hypoxia-ischemia.* Proc Natl Acad Sci U S A, 2011. **108**(46): p. 18802-7.
146. Liu, M., S. Doublie, and S.S. Wallace, *Neil3, the final frontier for the DNA glycosylases that recognize oxidative damage.* Mutat Res, 2013. **743-744**: p. 4-11.
147. Torisu, K., et al., *Hematopoietic tissue-specific expression of mouse Neil3 for endonuclease VIII-like protein.* J Biochem, 2005. **138**(6): p. 763-72.
148. Rolseth, V., et al., *Widespread distribution of DNA glycosylases removing oxidative DNA lesions in human and rodent brains.* DNA Repair (Amst), 2008. **7**(9): p. 1578-88.
149. Hildrestrand, G.A., et al., *Expression patterns of Neil3 during embryonic brain development and neoplasia.* BMC Neurosci, 2009. **10**: p. 45.
150. Yevshin, I., et al., *GTRD: a database of transcription factor binding sites identified by ChIP-seq experiments.* Nucleic Acids Res, 2017. **45**(D1): p. D61-D67.
151. Daily, K., et al., *MotifMap: integrative genome-wide maps of regulatory motif sites for model species.* BMC Bioinformatics, 2011. **12**: p. 495.
152. Xie, X., P. Rigor, and P. Baldi, *MotifMap: a human genome-wide map of candidate regulatory motif sites.* Bioinformatics, 2009. **25**(2): p. 167-74.
153. Kreutzer, D.A. and J.M. Essigmann, *Oxidized, deaminated cytosines are a source of C --> T transitions in vivo.* Proc Natl Acad Sci U S A, 1998. **95**(7): p. 3578-82.
154. Vooijs, M., J. Jonkers, and A. Berns, *A highly efficient ligand-regulated Cre recombinase mouse line shows that LoxP recombination is position dependent.* EMBO Rep, 2001. **2**(4): p. 292-7.
155. Chen, X., A. Pappo, and M.A. Dyer, *Pediatric solid tumor genomics and developmental pliancy.* Oncogene, 2015. **34**(41): p. 5207-15.

APPENDIX

Supplementary Material

Supplementary Table S1. Fold change values and associated P-values for each DNA repair gene included in the RT^2 Profiler PCR array.

Symbol	Embryonic Kidney Fold Change (comparing to adult kidney)	P-value (comparing to adult kidney)
Apex1	10.6295	0.000839
Apex2	4.1602	0.004169
Atm	2.061	0.054225
Atr	2.2815	0.009319
Atxn3	1.1251	0.966323
Brca1	24.59	0.000162
Brca2	7.1768	0.002343
Brip1	8.3013	0.002834
Ccnh	2.6027	0.012589
Ccno	0.6643	0.648675
Cdk7	5.0982	0.002982
Ddb1	2.4509	0.008761
Ddb2	3.4983	0.000034
Dmc1	3.8548	0.111203
Ercc1	4.6268	0.000447
Ercc2	1.9141	0.128101
Ercc3	5.5022	0.001004
Ercc4	1.4641	0.300542
Ercc5	2.3134	0.038097
Ercc6	2.7447	0.00856
Ercc8	2.271	0.057208
Exo1	34.7755	0.019745
Fen1	10.5074	0.01858
Lig1	28.5747	0.001224
Lig3	5.5919	0.003499
Lig4	2.6697	0.008114
Mgmt	1.9141	0.009647
Mlh1	3.8282	0.039664
Mlh3	0.8312	0.604044
Mms19	2.0849	0.062483
Mpg	3.0175	0.001569

Mre11a	3.0667	0.003511
Msh2	11.6587	0.014532
Msh3	1.7451	0.07426
Msh4	0.5599	0.560657
Msh5	1.0943	0.859842
Msh6	8.515	0.013548
Mutyh	11.6318	0.016968
Neil1	0.7596	0.544057
Neil2	0.5561	0.341552
Neil3	28.0514	0.003121
Nthl1	2.9759	0.013747
Ogg1	1.2894	0.103845
Parp1	4.7789	0.003536
Parp2	3.793	0.003625
Parp3	0.4253	0.239346
Pms1	2.0562	0.05736
Pms2	8.4561	0.000006
Pnkp	0.7492	0.390417
Polb	1.1096	0.822934
Pold3	4.4076	0.008083
Poll	1.9498	0.031352
Prkdc	1.6021	0.168439
Rad18	25.8722	0.000154
Rad21	3.3714	0.000592
Rad23a	1.6208	0.094769
Rad23b	2.1585	0.002455
Rad50	3.9908	0.007216
Rad51	50.5626	0.071733
Rad51c	4.9132	0.000395
Rad51b	24.8757	0.002358
Rad51d	0.7667	0.668549
Rad52	2.6512	0.080292
Rad54l	15.3837	0.003551
Rfc1	5.5277	0.00057
Rpa1	2.1634	0.064496
Rpa3	5.4264	0.084011
Slk	1.9453	0.021347
Smug1	1.1514	0.795024
Tdg	3.2266	0.008855
Top3a	2.5198	0.000601
Top3b	1.6396	0.063164

Trex1	3.8816	0.016992
Ung	27.1585	0.001891
Xab2	2.1585	0.048162
Xpa	1.1701	0.321335
Xpc	1.0401	0.869525
Xrcc1	3.3792	0.000737
Xrcc2	5.0747	0.001289
Xrcc3	2.4284	0.056838
Xrcc4	2.3457	0.009416
Xrcc5	1.9274	0.003558
Xrcc6	2.5491	0.049805
Xrcc6bp1	1	0.887347

This fold change value represents the normalized expression for the gene of interest in the embryonic kidney divided by its normalized expression in the adult kidney. Fold change values greater than 2.0 are indicated in red. Each P-value was calculated using a Student's t-test of the normalized expression for each gene in the embryonic versus the adult kidney samples. P-values less than 0.05 are indicated in red.

Reprinting Permissions

Reprinting Permission for Figure 1 (taken from [14])

Reprinted by permission from Springer Nature: Moritz, K.M., et al., *Factors influencing mammalian kidney development: implications for health in adult life.* Adv Anat Embryol Cell Biol, 2008. **196**: p. 1-78.